



1 **Microbial methanogenesis in the sulfate-reducing zone in sediments**

2 **from Eckernförde Bay, SW Baltic Sea**

3 Johanna Maltby^{1,2*}, Lea Steinle^{3,1}, Carolin R. Löscher^{4,1}, Hermann W. Bange¹, Martin A. Fischer⁵, Mark

4 Schmidt¹, Tina Treude^{1,6*}

5 ¹GEOMAR Helmholtz Centre for Ocean Research Kiel, Department of Marine Biogeochemistry, 24148

6 Kiel, Germany

7 ² Present Address: Natural Sciences Department, Saint Joseph's College, Standish, Maine 04084, USA

8 ³ Department of Environmental Sciences, University of Basel, 4056 Basel, Switzerland

9 ⁴ Nordic Center for Earth Evolution, University of Southern Denmark, 5230 Odense, Denmark

10 ⁵ Institute of Microbiology, Christian-Albrecht-University Kiel, 24118 Kiel, Germany

11 ⁶ Department of Earth, Planetary, and Space Sciences, Department of Atmospheric and Oceanic
12 Sciences, University of California, Los Angeles (UCLA), Los Angeles, California 90095-1567, USA

13

14 *Correspondence: jmaltby@sjcme.edu, ttreude@g.ucla.edu

15

16

17

18

19

20

21

22

23

24



25 Abstract

26 The presence of surface methanogenesis, located within the sulfate-reducing zone (0-30 centimeters
27 below seafloor, cmbsf), was investigated in sediments of the seasonally hypoxic Eckernförde Bay,
28 southwestern Baltic Sea. Water column parameters like oxygen, temperature and salinity together
29 with porewater geochemistry and benthic methanogenesis rates were determined in the sampling
30 area “Boknis Eck” quarterly from March 2013 to September 2014, to investigate the effect of
31 seasonal environmental changes on the rate and distribution of surface methanogenesis and to
32 estimate its potential contribution to benthic methane emissions. The metabolic pathway of
33 methanogenesis in the presence or absence of sulfate reducers and after the addition of a non-
34 competitive substrate was studied in four experimental setups: 1) unaltered sediment batch
35 incubations (net methanogenesis), 2) ^{14}C -bicarbonate labeling experiments (hydrogenotrophic
36 methanogenesis), 3) manipulated experiments with addition of either molybdate (sulfate reducer
37 inhibitor), 2-bromoethane-sulfonate (methanogen inhibitor), or methanol (non-competitive
38 substrate, potential methanogenesis), 4) addition of ^{13}C -labeled methanol (potential methylotrophic
39 methanogenesis). After incubation with methanol in the manipulated experiments, molecular
40 analyses were conducted to identify key functional methanogenic groups. Hydrogenotrophic
41 methanogenesis in sediments below the sulfate-reducing zone (> 30 cmbsf) was determined by ^{14}C -
42 bicarbonate radiotracer incubation in samples collected in September 2013.

43 Surface methanogenesis changed seasonally in the upper 30 cmbsf with rates increasing from March
44 ($0.2 \text{ nmol cm}^{-3} \text{ d}^{-1}$) to November ($1.3 \text{ nmol cm}^{-3} \text{ d}^{-1}$) 2013 and March ($0.2 \text{ nmol cm}^{-3} \text{ d}^{-1}$) to September
45 ($0.4 \text{ nmol cm}^{-3} \text{ d}^{-1}$) 2014, respectively. Its magnitude and distribution appeared to be controlled by
46 organic matter availability, C/N, temperature, and oxygen in the water column, revealing higher rates
47 in warm, stratified, hypoxic seasons (September/November) compared to colder, oxygenated
48 seasons (March/June) of each year. The majority of surface methanogenesis was likely driven by the
49 usage of non-competitive substrates (e.g., methanol and methylated compounds), to avoid
50 competition with sulfate reducers, as it was indicated by the 1000-3000-fold increase in potential
51 methanogenesis activity observed after methanol addition. Accordingly, competitive
52 hydrogenotrophic methanogenesis increased in the sediment only below the depth of sulfate
53 penetration (> 30 cmbsf). Members of the family *Methanosarcinaceae*, which are known for
54 methylotrophic methanogenesis, were detected by PCR using *Methanosarcinaceae*-specific primers
55 and are likely to be responsible for the observed surface methanogenesis.

56 The present study indicated that surface methanogenesis makes an important contribute to the
57 benthic methane budget of Eckernförde Bay sediments as it could directly feed into methane
58 oxidation above the sulfate-methane transition zone.



59 1. Introduction

60 After water vapor and carbon dioxide, methane is the most abundant greenhouse gas in the
61 atmosphere (e.g. Hartmann et al., 2013; Denman et al., 2007). Its atmospheric concentration
62 increased more than 150 % since preindustrial times, mainly through increased human activities such
63 as fossil fuel usage and livestock breeding (Hartmann et al., 2013; Wuebbles & Hayhoe, 2002;
64 Denman et al., 2007). Determining the natural and anthropogenic sources of methane is one of the
65 major goals for oceanic, terrestrial and atmospheric scientists to be able to predict further impacts
66 on the world's climate. The ocean is considered to be a modest natural source for atmospheric
67 methane (Wuebbles & Hayhoe, 2002; Reeburgh, 2007; EPA, 2010). However, research is still sparse
68 on the origin of the observed oceanic methane, which automatically leads to uncertainties in current
69 ocean flux estimations (Bange et al., 1994; Naqvi et al., 2010; Bakker et al., 2014).

70 Within the marine environment, the coastal areas (including estuaries and shelf regions) are
71 considered the major source for atmospheric methane, contributing up to 75 % to the global ocean
72 methane production (Bange et al., 1994). The major part of the coastal methane is produced during
73 microbial methanogenesis in the sediment, with probably only a minor part originating from
74 methane production within the water column (Bakker et al., 2014). However, the knowledge on
75 magnitude, seasonality and environmental controls of benthic methanogenesis is still limited.
76 In marine sediments, methanogenesis activity is mostly restricted to the sediment layers below
77 sulfate reduction, due to the successful competition of sulfate reducers with methanogens for the
78 mutual substrates acetate and hydrogen (H₂) (Oremland & Polcin, 1982; Crill & Martens, 1986;
79 Jørgensen, 2006). Methanogens produce methane mainly from using acetate (acetoclastic
80 methanogenesis) or H₂ and carbon dioxide (CO₂) (hydrogenotrophic methanogenesis). Competition
81 with sulfate reducers can be relieved through usage of non-competitive substrates (e.g. methanol or
82 methylated compounds, methylotrophic methanogenesis) (Cicerone & Oremland, 1988; Oremland &
83 Polcin, 1982). Coexistence of sulfate reduction and methanogenesis has been detected in a few
84 studies from organic-rich sediments, e.g., salt-marsh sediments (Oremland et al., 1982; Buckley et al.,
85 2008), coastal sediments (Holmer & Kristensen, 1994; Jørgensen & Parkes, 2010) or sediments in
86 upwelling regions (Pimenov et al., 1993; Ferdelman et al., 1997; Maltby et al., 2016), indicating the
87 importance of these environments for surface methanogenesis. So far, however, environmental
88 control mechanisms of surface methanogenesis remain elusive.

89 The coastal inlet Eckernförde Bay (southwestern Baltic Sea) is an excellent model environment to
90 study seasonal and environmental control mechanisms of benthic surface methanogenesis. Here,
91 the muddy sediments are characterized by high organic loading and high sedimentation rates
92 (Whiticar, 2002), which lead to anoxic conditions within the uppermost 0.1-0.2 centimeter below
93 seafloor (cmbsf) (Preisler et al., 2007). Seasonally hypoxic (dissolved oxygen < 63 µM) and anoxic



94 (dissolved oxygen = 0 μM) events in the bottom water of Eckernförde Bay (Lennartz et al., 2014)
95 provide ideal conditions for anaerobic processes at the sediment surface.

96 Sulfate reduction is the dominant pathway of organic carbon degradation in Eckernförde Bay
97 sediments in the upper 30 cmbsf, followed by methanogenesis in deeper sediment layers where
98 sulfate is depleted (> 30 cmbsf) (Whiticar 2002; Treude et al. 2005; Martens et al. 1998). This deep
99 methanogenesis can be intense and often leads to methane oversaturation in the porewater below
100 50 cm sediment depth, resulting in gas bubble formation (Abegg & Anderson, 1997; Whiticar, 2002;
101 Thießen et al., 2006). Thus, methane is transported from the methanogenic zone (> 30 cmbsf) to the
102 surface sediment by both molecular diffusion and advection via rising gas bubbles (Wever et al.,
103 1998; Treude et al., 2005a). Although upward diffusing methane is mostly retained by anaerobic
104 oxidation of methane (AOM) (Treude et al. 2005), a major part is reaching the sediment-water
105 interface through gas bubble transport (Treude et al. 2005; Jackson et al. 1998), resulting in a
106 supersaturation of the water column with respect to atmospheric methane concentrations (Bange et
107 al., 2010). The Time Series Station "Boknis Eck" in the Eckernförde Bay is a known site of methane
108 emissions into the atmosphere throughout the year due to this supersaturation of the water column
109 (Bange et al., 2010).

110 The source for benthic and water column methane was seen in deep methanogenesis (> 30 cmbsf)
111 below the penetration of sulfate (Whiticar, 2002), however, coexistence of sulfate reduction and
112 methanogenesis has been postulated (Whiticar, 2002; Treude et al., 2005a). Still, the magnitude and
113 environmental controls of surface methanogenesis is poorly understood, even though it may make a
114 measurable contribution to benthic methane emissions given its short diffusion distance to the
115 sediment-water interface (Knittel & Boetius, 2009). Production of methane within the sulfate
116 reduction zone of Eckernförde Bay surface sediments could further explain peaks of methane
117 oxidation observed in top sediment layers, which was previously attributed to methane transported
118 to the surface via rising gas bubbles (Treude et al., 2005a).

119 In the present study, we investigated surface sediment (< 30 cmbsf, on a seasonal basis), deep
120 sediment (> 30 cmbsf, on one occasion), and the water column (on a seasonal basis) at the Time
121 Series Station "Boknis Eck" in Eckernförde Bay, to validate the existence of surface methanogenesis
122 and its potential contribution to benthic methane emissions. Water column parameters like oxygen,
123 temperature, and salinity together with porewater geochemistry and benthic methanogenesis were
124 measured over a course of 2 years. In addition to seasonal rate measurements, inhibition and
125 stimulation experiments, stable isotope probing, and molecular analysis were carried out to find out
126 if surface methanogenesis 1) is controlled by environmental parameters, 2) shows seasonal
127 variability, 3) is based on non-competitive substrates with a special focus on methylothrophic
128 methanogens.



129 2. Material and Methods

130 2.1 Study site

131 Samples were taken at the Time Series Station "Boknis Eck" (BE, 54°31.15 N, 10°02.18 E;
132 www.bokniseck.de) located at the entrance of Eckernförde Bay in the southwestern Baltic Sea with a
133 water depth of about 28 m (map of sampling site can be found in e.g. Hansen et al., (1999)). From
134 mid of March until mid of September the water column is strongly stratified due to the inflow of
135 saltier North Sea water and a warmer and fresher surface water (Bange et al., 2011). Organic matter
136 degradation in the deep layers causes pronounced hypoxia (March-Sept) or even anoxia
137 (August/September) (Smetacek, 1985; Smetacek et al., 1984). The source of organic material is
138 phytoplankton blooms, which occur regularly in spring (February-March) and fall (September-
139 November) and are followed by pronounced sedimentation of organic matter (Bange et al., 2011). To
140 a lesser extent, phytoplankton blooms and sedimentation are also observed during the summer
141 months (July/August) (Smetacek et al., 1984). Sediments at BE are generally classified as soft, fine-
142 grained muds (< 40 µm) with a carbon content of 3 to 5 wt% (Balzer et al., 1986). The bulk of organic
143 matter in Eckernförde Bay sediments originates from marine plankton and macroalgal sources (Orsi
144 et al., 1996), and its degradation leads to production of free methane gas (Wever & Fiedler, 1995;
145 Abegg & Anderson, 1997; Wever et al., 1998). The oxygen penetration depth is limited to the upper
146 few millimeters when bottom waters are oxic (Preisler et al., 2007). Reducing conditions within the
147 sulfate reduction zone lead to a dark grey/black sediments color with a strong hydrogen sulfur odor
148 in the upper meter of the sediment and dark olive-green color the deeper sediment layers (> 1 m)
149 (Abegg & Anderson, 1997).

150 2.2 Water column and sediment sampling

151 Sampling was done on a seasonal basis during the years of 2013 and 2014. One-Day field trips with
152 either F.S. Alkor (cruise no. AL410), F.K. Littorina or F.B. Polarfuchs were conducted in March, June,
153 and September of each year. In 2013, additional sampling was conducted in November. At each
154 sampling month, water profiles of temperature, salinity, and oxygen concentration (optical sensor,
155 RINKO III, detection limit= 2 µM) were measured with a CTD (Hydro-Bios). In addition, water samples
156 for methane concentration measurements were taken at 25 m water depth with a 6-Niskin bottle (4
157 Liter each) rosette attached to the CTD (Table 1). Complementary samples for water column
158 chlorophyll were taken at 25 m water depth with the CTD-rosette within the same months during
159 standardized monthly sampling cruises to Boknis Eck organized by GEOMAR.
160 Sediment cores were taken with a miniature multicorer (MUC, K.U.M. Kiel), holding 4 core liners
161 (length= 60 cm, diameter= 10 cm) at once. The cores had an average length of ~ 30 cm and were



162 stored at 10°C in a cold room (GEOMAR) until further processing (normally within 1-3 days after
163 sampling).

164 In September 2013, a gravity core was taken in addition to the MUC cores. The gravity core was
165 equipped with an inner plastic bag (polyethylene; diameter: 13 cm). After core recovery (330 cm
166 total length), the polyethylene bag was cut open at 12 different sampling depths resulting in intervals
167 of 30 cm and sampled directly on board for sediment porewater geochemistry (see Sect. 2.4),
168 sediment methane (see Sect. 2.5), sediment solid phase geochemistry (see Sect. 2.6), and microbial
169 rate measurements for hydrogenotrophic methanogenesis as described in section 2.8.

170 2.3 Water column parameters

171 At each sampling month, water samples for methane concentration measurements were taken at 25
172 m water depth in triplicates. Therefore, three 25 ml glass vials were filled bubble free directly after
173 CTD-rosette recovery and closed with butyl rubber stoppers. Samples were killed with saturated
174 mercury chloride solution and stored at room temperature until further treatment.

175 Concentrations of dissolved methane (CH₄) were determined by headspace gas chromatography as
176 described in Bange et al. (2010). Calibration for CH₄ was done by a two-point calibration with known
177 methane concentrations before the measurement of headspace gas samples, resulting in an error of
178 < 5 %.

179 Water samples for chlorophyll concentration were taken by transferring the complete water volume
180 (from 25 m water depth) from one water sampler into a 4.5 L Nalgene bottle, from which then
181 approximately 0.7-1 L (depending on the plankton content) were filtrated back in the GEOMAR
182 laboratory using GF/F filter (Whatman, 25 mm diameter, 8 µM pores size). Dissolved chlorophyll a
183 concentrations were determined using the fluorometric method by Welschmeyer (1994) with an
184 error < 10 %.

185 2.4 Sediment porewater geochemistry

186 Porewater was extracted from sediment within 24 hours after core retrieval using nitrogen (N₂) pre-
187 flushed rhizons (0.2 µm, Rhizosphere Research Products, Seeberg-Elverfeldt et al., 2005). In MUC
188 cores, rhizons were inserted into the sediment in 2 cm intervals through pre-drilled holes in the core
189 liner. In the gravity core, rhizons were inserted into the sediment in 30 cm intervals directly after
190 retrieval.

191 Extracted porewater from MUC and gravity cores was immediately analyzed for sulfide using
192 standardized photometric methods (Grasshoff et al., 1999).

193 Sulfate concentrations were determined using ion chromatography (Methrom 761). Analytical
194 precision was < 1 % based on repeated analysis of IAPSO seawater standards (dilution series) with an



195 absolute detection limit of 1 μM corresponding to a detection limit of 30 μM for the undiluted
196 sample.

197 For analysis of dissolved inorganic carbon (DIC), 1.8 ml of porewater was transferred into a 2 ml glass
198 vial, fixed with 10 μl saturated HgCl_2 solution and crimp sealed. DIC concentration was determined
199 as CO_2 with a multi N/C 2100 analyzer (Analytik Jena) following the manufacturer's instructions.
200 Therefore, the sample was acidified with phosphoric acid and the outgassing CO_2 was measured. The
201 detection limit was 20 μM with a precision of 2-3 %.

202 2.5 Sediment methane concentrations

203 In March 2013, June 2013 and March 2014, one MUC core was sliced in 1 cm intervals until 6 cmbsf,
204 followed by 2 cm intervals until the end of the core. At the other sampling months, the MUC core
205 was sliced in 1 cm intervals until 6 cmbsf, followed by 2 cm intervals until 10 cmbsf and 5 cm intervals
206 until the end of the core.

207 Per sediment depth (in MUC and gravity cores), 2 cm^3 of sediment were transferred into a 10 ml-
208 glass vial containing 5 ml NaOH (2.5 %) for determination of sediment methane concentration per
209 volume of sediment. The vial was quickly closed with a butyl septum, crimp-sealed and shaken
210 thoroughly. The vials were stored upside down at room temperature until measurement via gas
211 chromatography. Therefore, 100 μl of headspace was removed from the gas vials and injected into a
212 Shimadzu gas chromatograph (GC-2014) equipped with a packed Haysep-D column and a flame
213 ionization detector. The column temperature was 80°C and the helium flow was set to 12 ml min^{-1} .
214 CH_4 concentrations were calibrated against CH_4 standards (Scotty gases). The detection limit was 0.1
215 ppm with a precision of 2 %.

216 2.6 Sediment solid phase geochemistry

217 Following the sampling for CH_4 , the same cores described under section 2.5 were used for the
218 determination of the sediment solid phase geochemistry, i.e. porosity, particulate organic carbon
219 (POC) and particulate organic nitrogen (PON).

220 Sediment porosity of each sampled sediment section was determined by the weight difference of 5
221 cm^3 wet sediment after freeze-drying for 24 hours. Dried sediment samples were then used for
222 analysis of particulate organic carbon (POC) and particulate organic nitrogen (PON) with a Carlo-Erba
223 element analyzer (NA 1500). The detection limit for C and N analysis was < 0.1 dry weight percent (%)
224 with a precision of < 2 %.

225 2.7 Sediment methanogenesis

226 2.7.1 Methanogenesis in MUC cores

227 At each sampling month, three MUC cores were sliced in 1 cm intervals until 6 cmbsf, in 2 cm
228 intervals until 10 cmbsf, and in 5 cm intervals until the bottom of the core. Every sediment layer was



229 transferred to a separate beaker and quickly homogenized before sub-sampling. The exposure time
230 with air, i.e. oxygen, was kept to a minimum. Sediment layers were then sampled for determination
231 of net methanogenesis (defined as the sum of total methane production and consumption, including
232 all available methanogenic substrates in the sediment), hydrogenotrophic methanogenesis
233 (methanogenesis based on the substrates CO_2/H_2), and potential methanogenesis (methanogenesis
234 at ideal conditions, i.e. no lack of nutrients) as described in the following sections.

235 ***Net methanogenesis***

236 Net methanogenesis was determined with sediment slurry experiments by measuring the headspace
237 methane concentration over time. Per sediment layer, triplicates of 5 cm^3 of sediment were
238 transferred into N_2 -flushed sterile glass vials (30 ml) and mixed with 5 ml filtered bottom water. The
239 slurry was repeatedly flushed with N_2 to remove residual methane and to ensure complete anoxia.
240 Slurries were incubated in the dark at in-situ temperature, which varied at each sampling date (Table
241 1). Headspace samples (0.1 ml) were taken out every 3-4 days over a time period of 4 weeks and
242 analyzed on a Shimadzu GC-2104 gas chromatograph (see Sect. 2.5). Net methanogenesis rates were
243 determined by the linear increase of the methane concentration over time (minimum of 6 time
244 points).

245 ***Hydrogenotrophic methanogenesis***

246 To determine hydrogenotrophic methanogenesis, radioactive sodium bicarbonate ($\text{NaH}^{14}\text{CO}_3$) was
247 added to the sediment.
248 Per sediment layer, sediment was sampled in triplicates with glass tubes (5 mL) which were closed
249 with butyl rubber stoppers on both ends according to (Treude et al. 2005). Through the stopper,
250 $\text{NaH}^{14}\text{CO}_3$ (dissolved in water, injection volume 6 μl , activity 222 kBq, specific activity = 1.85-2.22
251 GBq/mmol) was injected into each sample and incubated for three days in the dark at in-situ
252 temperature (Table 1). To stop bacterial activity, sediment was transferred into 50 ml glass-vials filled
253 with 20 ml sodium hydroxide (2.5 % w/w), closed quickly with rubber stoppers and shaken
254 thoroughly. Five controls were produced from various sediment depths by injecting the radiotracer
255 directly into the NaOH with sediment.
256 The production of ^{14}C -methane was determined with the slightly modified method by Treude et al.,
257 (2005) used for the determination of anaerobic oxidation of methane. The method was identical,
258 except no unlabeled methane was determined by gas chromatography. Instead, DIC values were
259 used to calculate hydrogenotrophic methane production.

260 ***Potential methanogenesis in manipulated experiments***

261 To examine the interaction between sulfate reduction and methanogenesis, inhibition and
262 stimulation experiments were carried out. Therefore, every other sediment layer was sampled



263 resulting in the following examined six sediment layers: 0-1 cm, 2-3 cm, 4-5 cm, 6-8 cm, 10-15 cm
264 and 20-25 cm. From each layer, sediment slurries were prepared by mixing 5 ml sediment in a 1:1
265 ratio with adapted artificial seawater medium (salinity 24, Widdel & Bak, 1992) in N₂-flushed, sterile
266 glass vials before further manipulations.

267 In total, four different treatments, each in triplicates, were prepared per depth: 1) with sulfate
268 addition (17 mM), 2) with sulfate (17 mM) and molybdate (22 mM) addition, 3) with sulfate (17 mM)
269 and 2-bromoethane-sulfonate (BES, 60 mM) addition, and 4) with sulfate (17 mM) and methanol (10
270 mM) addition. From here on, the following names are used to describe the different treatments,
271 respectively: 1) control treatment, 2) molybdate treatment, 3) BES treatment, and 4) methanol
272 treatment. Control treatments feature the natural sulfate concentrations occurring in surface
273 sediments of the sampling site. Molybdate was used as an enzymatic inhibitor for sulfate reduction
274 (Oremland & Capone, 1988) and BES was used as an inhibitor for methanogenic archaea (Hoehler et
275 al., 1994). Methanol is a known non-competitive substrate, which is used by methanogens but not by
276 sulfate reducers (Oremland & Polcin, 1982), thus it is suitable to examine non-competitive
277 methanogenesis. Treatments were incubated at the respective in-situ temperature (Table 1) in the
278 dark.

279 ***Potential methylotrophic methanogenesis from methanol using stable isotope probing***

280 One additional experiment was conducted with sediments from September 2014 by adding ¹³C-
281 labelled methanol to investigate the production of ¹³C-labelled methane. Three cores were stored at
282 1°C after the September 2014 cruise until further processing ~ 3.5 months later. The low storage
283 temperature and the fast oxygen consumption in the enclosed supernatant water (i.e., exclusion of
284 bioturbation by macrofauna) led to slowed microbial activity and preserved the sediments for
285 potential methanogenesis measurements.

286 Sediment cores were sliced in 2 cm intervals and the upper 0-2 cmbsf sediment layer of all three
287 cores was combined in a beaker and homogenized. Then, sediment slurries were prepared by mixing
288 5 cm⁻³ of sediment with 5 ml of artificial seawater medium in N₂-flushed, sterile glass vials (30 ml).
289 Then, methanol was added to the slurry with a final concentration of 10 mM (see Sect. 2.7.3), but
290 this time the methanol was enriched with ¹³C-labelled methanol in a ratio of 1:1000 between ¹³C-
291 labelled (99.9 % ¹³C) and non-labelled methanol mostly consisting of ¹²C (manufacturer: Roth). In
292 total, 54 vials were prepared for nine different sampling time points during a total incubation time of
293 37 days. All vials were incubated at 13°C (in situ temperature in September 2014) in the dark. At each
294 sampling point, six vials were stopped: one set of triplicates were used for headspace methane and
295 carbon dioxide determination and a second set of triplicates were used for porewater analysis.
296 Headspace methane and carbon dioxide concentrations (volume 100 µl) were determined on a
297 Shimadzu gas chromatograph (GC-2014) equipped with a packed Haysep-D column a flame ionization



298 detector and a methanizer. The methanizer (reduced nickel) reduces carbon dioxide with hydrogen
299 to methane at a temperature of 400°C. The column temperature was 80°C and the helium flow was
300 set to 12 ml min⁻¹. Methane concentrations (including reduced CO₂) were calibrated against methane
301 standards (Scotty gases). The detection limit was 0.1 ppm with a precision of 2 %.
302 Analyses of ¹³C/¹²C-ratios of methane and carbon dioxide were conducted after headspace
303 concentration measurements by using a continuous flow combustion gas chromatograph (Trace
304 Ultra, Thermo Scientific), which was coupled to an isotope ratio mass spectrometer (MAT253,
305 Thermo Scientific). The isotope ratios of methane and carbon dioxide given in the common delta-
306 notation ($\delta^{13}\text{C}$ in permill) are reported relative to Vienna Pee Dee Belemnite (VPDB) standard.
307 Isotope precision was +/- 0.5 ‰, when measuring near the detection limit of 10 ppm.
308 For porewater analysis of methanol concentration and isotope composition, each sediment slurry of
309 the triplicates was transferred into argon-flushed 15 ml centrifuge tubes and centrifuged for 6
310 minutes at 4500 rpm. Then 1 ml filtered (0.2 μm) porewater was transferred into N₂-flushed 2 ml
311 glass vials for methanol analysis, crimp sealed and immediately frozen at -20 °C. Methanol
312 concentrations and isotope composition were determined via high performance liquid
313 chromatography-ion ratio mass spectrometry (HPLC-IRMS, Thermo Fisher Scientific) at the MPI
314 Marburg. The detection limit was 50 μM with a precision of 0.3‰.

315 2.7.2 Methanogenesis in the gravity core

316 Ex situ hydrogenotrophic methanogenesis was determined in a gravity core taken September 2013. The
317 pathway is thought to be the main methanogenic pathway in the deep sediment layers (below
318 sulfate penetration) in Eckernförde Bay (Whiticar, 2002). Hydrogenotrophic methanogenesis was
319 determined using ¹⁴C-bicarbonate. At every sampled sediment depth (12 depths in 30 cm intervals),
320 triplicate glass tubes (5 mL) were inserted directly into the sediment. Tubes were filled bubble-free
321 with sediment and closed with butyl rubber stoppers on both ends according to (Treude et al. 2005).
322 Methods following sampling were identical as described in 2.7.2.

323 2.8 Molecular analysis

324 In September 2014, additional samples were prepared for the methanol treatment of the 0-1 cmbsf
325 horizon during the potential methanogenesis experiment described in 2.7.3 to detect and quantify
326 the presence of methanogens in the sediment. Therefore, additional 15 vials were prepared with
327 addition of methanol as described in 2.7.3 for five different time points (day 1 (= t₀), day 8, day 16,
328 day 22, and day 36) and stopped at each time point by transferring sediment from the triplicate
329 slurries into whirl-packs (Nasco), which then were immediately frozen at -20°C. DNA was extracted
330 from ~500 mg of sediment using the FastDNA® SPIN Kit for Soil (Biomedical). Quantitative real-time
331 polymerase chain reaction (qPCR) technique using TaqMan probes and TaqMan chemistry (Life



332 Technologies) was used for the detection of methanogens on a ViiA7 qPCR machine (Life
333 Technologies). Primer and Probe sets as originally published by Yu et al. (2005) were applied to
334 quantify the orders *Methanobacteriales*, *Methanosarcinales* and *Methanomicrobiales* along with the
335 two families *Methanosarcinaceae* and *Methanosaetaceae* within the order *Methanosarcinales*. In
336 addition, a universal primer set for detection of the domain *Archaea* was used (Yu et al. 2005).
337 Absolut quantification of the 16S rDNA from the groups mentioned above was performed with
338 standard dilution series. The standard concentration reached from 10^8 to 10^1 copies per μL .
339 Quantification of the standards and samples was performed in duplicates. Reaction was performed in
340 a final volume of 12.5 μL containing 0.5 μL of each Primer ($10\text{pmol } \mu\text{L}^{-1}$, MWG), 0.25 μL of the
341 respective probe ($10\text{ pmol } \mu\text{L}^{-1}$, Life Technologies), 4 μL H₂O (Roth), 6.25 μL TaqMan Universal Master
342 Mix II (Life Technologies) and 1 μL of sample or standard. Cycling conditions started with initial
343 denaturation and activation step for 10 min at 95°C, followed by 45 cycles of 95 °C for 15 sec, 56°C
344 for 30 sec and 60°C for 60 sec. Non-template controls were run in duplicates with water instead of
345 DNA for all primer and probe sets, and remained without any detectable signal after 45 cycles.

346 2.9 Statistical Analysis

347 To determine possible environmental controlling parameters on surface methanogenesis, a Principle
348 Component Analysis (PCA) was applied according to the approach described in Gier et al.(2016).
349 Prior to PCA, the dataset was transformed into ranks to assure the same data dimension.
350 In total, two PCAs were conducted. The first PCA was used to test the relation of parameters in the
351 surface sediment (integrated methanogenesis (0-5 cm, $\text{mmol m}^{-2} \text{d}^{-1}$), POC content (average value
352 from 0-5 cmbsf, wt %), C/N (average value from 0-5 cmbsf, molar) and the bottom water (25 m water
353 depth) (oxygen (μM), temperature (°C), salinity (PSU), chlorophyll ($\mu\text{g L}^{-1}$), methane (nM)). The
354 second PCA was applied on depth profiles of sediment surface methanogenesis ($\text{nmol cm}^{-3} \text{d}^{-1}$),
355 sediment depth (cm), sediment POC content (wt%), sediment C/N ratio (molar), and sampling month
356 (one value per depth profile at a specific month, the later in the year the higher the value).
357 For each PCA, biplots were produced to view data from different angles and to graphically determine
358 a potential positive, negative or zero correlation between methanogenesis rates and the tested
359 variables.

360 3. Results

361 3.1 Water column parameters

362 From March 2013 to September 2014, the water column had a pronounced temporal and spatial
363 variability of temperature, salinity, and oxygen (Fig. 1 and 2). In 2013, temperature of the upper
364 water column increased from March (1°C) to September (16°C), but decreased again in November



365 (11°C). The temperature of the lower water column increased from March 2013 (2°C) to November
366 2013 (12°C). In 2014, lowest temperatures of the upper and lower water column were reached in
367 March (4°C). Warmer temperatures of the upper water column were observed in June and
368 September (around 17°C), while the lower water column peaked in September (13°C).
369 Salinity increased over time during 2013, showing the highest salinity of the upper and lower water
370 column in November (18 and 23 PSU, respectively). In 2014, salinity of the upper water column was
371 highest in March and September (both 17 PSU), and lowest in June (13 PSU). The salinity of the lower
372 water column increased from March 2014 (21 PSU) to September 2014 (25 PSU).
373 In both years, June and September showed the most pronounced vertical gradient of temperature
374 and salinity, featuring a pycnocline at around ~14 m water depth.
375 Summer stratification was also seen in the O₂ profiles, which showed O₂ depleted conditions (O₂ <
376 150 μM) in the lower water column from June to September in both years, reaching concentrations
377 below 1- 2 μM (detection limit of CTD sensor) in September of both years (Fig. 1 and 2). The water
378 column was completely ventilated, i.e. homogenized, in March of both years with O₂ concentrations
379 of 300-400 μM down to the sea floor at about 28 m.
380

381 3.2 Sediment geochemistry in MUC cores

382 Sediment porewater and solid phase geochemistry results for the years 2013 and 2014 are shown in
383 Fig. 1 and 2, respectively.
384 Sulfate concentrations at the sediment surface ranged between 15-20 mM. Concentration decreased
385 with depth at all sampling months but was never fully depleted until the bottom of the core (18-29
386 cmbsf, between 2 and 7 mM sulfate). November 2013 showed the strongest decrease from ~20 mM
387 at the top to ~2 mM at the bottom of the core (27 cmbsf).
388 Opposite to sulfate, methane concentration increased with sediment depth in all sampling months
389 (Fig. 1 and 2). Over the course of a year (i.e. March to November in 2013, and March to September in
390 2014), maximum methane concentration increased, reaching the highest concentration in November
391 2013 (~1 mM at 26 cmbsf) and September 2014 (0.2 mM at 23 cmbsf), respectively. Simultaneously,
392 methane profiles became steeper, revealing higher methane concentrations at shallower sediment
393 depth late in the year. Magnitudes of methane concentrations were similar in the respective months
394 of 2013 and 2014.
395 In all sampling months, sulfide concentration increased with sediment depth (Fig. 1 and 2). Similar to
396 methane, sulfide profiles revealed higher sulfide concentrations at shallower sediment depth
397 together with higher peak concentrations over the course the sampled months in each sampling
398 year. Accordingly, November 2013 (10.5 mM at 15 cmbsf) and in September 2014 (2.8 mM at 15
399 cmbsf) revealed the highest sulfide concentrations, respectively. September 2014 was the only



400 sampling month showing a pronounced decrease in sulfide concentration from 15 cmbsf to 21 cmbsf
401 of over 50 %.

402 DIC concentrations increased with increasing sediment depth at all sampling months. Concomitant
403 with highest sulfide concentrations, highest DIC concentration was detected in November 2013 (26
404 mM at 27 cmbsf). At the surface, DIC concentrations ranged between 2-3 mM at all sampling
405 months. In June of both years, DIC concentrations were lowest at the deepest sampled depth
406 compared to the other sampling months (16 mM in 2013, 13 mM in 2014).

407 At all sampling months, POC profiles scattered around 5 ± 0.9 wt % with depth. Only in November
408 2013, June 2014 and September 2014, POC content exceeded 5 wt % in the upper 0-1 cmbsf (5.9, 5.2
409 and 5.3 wt %, respectively) with the highest POC content in November 2013. Also in November 2013,
410 surface C/N ratio was lowest of all sampling months (8.6). In general, C/N ratio increased with depth
411 in both years with values around 9 at the surface and values around 10-11 at the deepest sampled
412 sediment depths.

413 3.3 Sediment geochemistry in gravity cores

414 Results from sediment porewater and solid phase geochemistry in the gravity core from September
415 2013 are shown in Fig. 3. Please note that the sediment depth of the gravity core was corrected by
416 comparing the sulfate concentrations at 0 cmbsf in the gravity core with the corresponding sulfate
417 concentration and depth in the MUC core from September 2013 (Fig. 1). The soft surface sediment is
418 often lost during the gravity coring procedure. Through this correction the topmost layer of the
419 gravity core was set at a depth of 14 cmbsf.

420 Porewater sulfate concentration in the gravity core decreased with depth (i.e. below 0.1 mM at 107
421 cmbsf) and stayed below 0.1 mM until 324 cmbsf. Sulfate increased slightly (1.9 mM) at the bottom
422 of the core (345 cmbsf). In concert with sulfate, also methane, sulfide, DIC, POC and C/N profiles
423 showed distinct alteration in the profile at 345 cmbsf (see below, Fig. 3). As fluid seepage has not
424 been observed at the Boknis Eck station (Schlüter et al., 2000), these alterations could either indicate
425 a change in sediment properties or result from a sampling artifact from the penetration of seawater
426 through the core catcher into the deepest sediment layer. The latter process is, however, not
427 expected to considerably affect sediment solid phase properties (POC and C/N), and we therefore
428 dismissed this hypothesis.

429 Methane concentration increased steeply with depth reaching a maximum of 4.8 mM at 76 cmbsf.
430 Concentration stayed around 4.7 mM until 262 cmbsf, followed by a slight decrease until 324 cmbsf
431 (2.8 mM). From 324 cmbsf to 345 cmbsf methane increased again (3.4 mM).

432 Both sulfide and DIC concentrations increased with depth, showing a maximum at 45 cmbsf (~ 5 mM)
433 and 345 cmbsf (~ 1 mM), respectively. While sulfide decreased after 45 cmbsf to a minimum of ~ 300
434 μ M at 324 cmbsf, it slightly increased again to ~ 1 mM at 345 cmbsf. In accordance, DIC



435 concentrations showed a distinct decrease between 324 cmbsf to 345 cmbsf (from 45 mM to 39
436 mM).
437 While POC concentrations varied around 5 wt % throughout the core, C/N ratio slightly increased
438 with depth, revealing the lowest ratio at the surface (~3) and the highest ratio at the bottom of the
439 core (~13). However, both POC and C/N showed a distinct increase from 324 cmbsf to 345 cmbsf.
440

441 **3.4 Methanogenesis activity in MUC cores**

442 **3.4.1 Net methanogenesis**

443 Net methanogenesis activity was detected throughout the cores at all sampling months (Fig. 1 and 2).
444 Activity measured in MUC cores increased over the course of the year in 2013 and 2014 (that is:
445 March to November in 2013 and March to September in 2014) with lower rates mostly $< 0.1 \text{ nmol}$
446 $\text{cm}^{-3} \text{d}^{-1}$ in March and higher rates $> 0.2 \text{ nmol cm}^{-3} \text{d}^{-1}$ in November 2013 and September 2014,
447 respectively. In general, November 2013 revealed highest net methanogenesis rates ($1.3 \text{ nmol cm}^{-3} \text{d}^{-1}$
448 at 1-2 cmbsf). Peak rates were detected at the sediment surface (0-1 cmbsf) at all sampling months
449 except for September 2013 where the maximum rates were situated between 10-15 cmbsf. In
450 addition to the surface peaks, net methanogenesis showed subsurface (= below 1 cmbsf until 30
451 cmbsf) maxima at all sampling months, but with alternating depths (between 10 and 25 cmbsf).
452 Comparison of integrated net methanogenesis rates (0-25 cmbsf) revealed highest rates in
453 September and November 2013 and lowest rates in March 2014 (Fig. 4). A trend of increasing areal
454 net methanogenesis rates from March to September was observed in both years.

455 **3.4.2 Hydrogenotrophic methanogenesis**

456 Hydrogenotrophic methanogenesis activity determined by ^{14}C -bicarbonate incubations of MUC cores
457 is shown in Fig. 1 and 2. In 2013, maximum activity ranged between $0.01\text{-}0.2 \text{ nmol cm}^{-3} \text{d}^{-1}$, while in
458 2014 maxima ranged only between 0.01 and $0.05 \text{ nmol cm}^{-3} \text{d}^{-1}$. In comparison, maximum
459 hydrogenotrophic methanogenesis was up to two orders of magnitude lower compared to net
460 methanogenesis. Only in March 2013 both activities reached a similar range.
461 Overall, hydrogenotrophic methanogenesis increased with depth in March, September, and
462 November 2013 and in March, June, and September 2014. In June 2013, activity decreased with
463 depth, showing the highest rates in the upper 0-5 cmbsf and the lowest at the deepest sampled
464 depth.
465 Concomitant with integrated net methanogenesis, integrated hydrogenotrophic methanogenesis
466 rates (0-25 cmbsf) were high in September 2013, with slightly higher rates in March 2013 (Fig. 4).
467 Lowest areal rates of hydrogenotrophic methanogenesis were seen in June of both years.



468 Hydrogenotrophic methanogenesis activity in the gravity core is shown in Fig. 3. Highest activity (~
469 $0.7 \text{ nmol cm}^{-3} \text{ d}^{-1}$) was measured at 45 cmbsf and 138 cmbsf, followed by a decrease with increasing
470 sediment depth reaching $0.01 \text{ nmol cm}^{-3} \text{ d}^{-1}$ at the deepest sampled depth (345 cmbsf).

471 **3.4.3 Potential methanogenesis in manipulated experiments**

472 Potential methanogenesis rates in manipulated experiments included either the addition of
473 inhibitors (molybdate for inhibition of sulfate reduction or BES for inhibition of methanogenesis) or
474 the addition of a non-competitive substrate (methanol). Control treatments were run with neither
475 the addition of inhibitors nor the addition of methanol.

476 *Controls.* Potential methanogenesis activity in the control treatments was below $0.5 \text{ nmol cm}^{-3} \text{ d}^{-1}$
477 from March 2014 to September 2014 (Fig. 5). Only in November 2013, control rates exceeded 0.5
478 $\text{nmol cm}^{-3} \text{ d}^{-1}$ below 6 cmbsf. While rates increased with depth in November 2013 and June 2014,
479 they decreased with depth at the other two sampling months.

480 *Molybdate.* Peak potential methanogenesis rates in the molybdate treatments were found in the
481 uppermost sediment interval (0-1 cmbsf) at almost every sampling month with rates being 3-30
482 times higher compared to the control treatments ($< 0.5 \text{ nmol cm}^{-3} \text{ d}^{-1}$). In November 2013, potential
483 methanogenesis showed two maxima (0-1 and 10-15 cmbsf). Highest measured rates were found in
484 September 2014 ($\sim 6 \text{ nmol cm}^{-3} \text{ d}^{-1}$), followed by November 2013 ($\sim 5 \text{ nmol cm}^{-3} \text{ d}^{-1}$).

485 *BES.* Profiles of potential methanogenesis in the BES treatments were similar to the controls mostly
486 in the lower range $< 0.5 \text{ nmol cm}^{-3} \text{ d}^{-1}$. Only in November 2013 rates exceeded $0.5 \text{ nmol cm}^{-3} \text{ d}^{-1}$.
487 Rates increased with depth at all sampling months, except for September 2014, where highest rates
488 were found at the sediment surface (0-1 cmbsf).

489 *Methanol.* At all sampling months, potential rates in the methanol treatments were three orders of
490 magnitude higher compared to the control treatments ($< 0.5 \text{ nmol cm}^{-3} \text{ d}^{-1}$). Except for November
491 2013, potential methanogenesis rates in the methanol treatments were highest in the upper 0-5
492 cmbsf and decreased with depth. In November 2013, highest rates were detected at the deepest
493 sampled depth (20-25 cmbsf).

494

495 **3.4.4 Potential methanogenesis determined from ^{13}C -labelled methanol**

496 The concentration of methanol in the sediment decreased sharply in the first 2 weeks from $\sim 8 \text{ mM}$ at
497 day 1 to 0.5 mM at day 13 (Fig. 6). At day 17, methanol was below the detection limit. In the first 2
498 weeks, residual methanol was enriched with ^{13}C , reaching $\sim 200 \text{ ‰}$ at day 13.

499 Over the same time period, the concentration of methane increased from 2 ppmv at day 1 to \sim
500 $66,000 \text{ ppmv}$ at day 17 and stayed around that value until the end of the total incubation time (until
501 day 37) (Fig. 6). The carbon isotopic signature of methane ($\delta^{13}\text{C}_{\text{CH}_4}$) showed a clear enrichment of the
502 heavier isotope ^{13}C (Table 3) from day 9 to 17 (no methane was detectable at day 1). After day 17,



503 $\delta^{13}\text{C}_{\text{CH}_4}$ stayed around 13‰ until the end of the incubation. The concentration of CO_2 in the
504 headspace increased from ~ 8900 ppmv at day 1 to $\sim 29,000$ ppmv at day 20 and stayed around
505 30,000 ppmv until the end of the incubation (Fig. 6). Please note, that the major part of CO_2 was
506 dissolved in the porewater, thus the CO_2 concentration in the headspace does not show the total CO_2
507 concentration in the system. CO_2 in the headspace was enriched with ^{13}C during the first 2 weeks
508 (from -16.2 to -7.3 ‰) but then stayed around -11 ‰ until the end of the incubation.

509 3.5 Molecular analysis of benthic methanogens

510 In September 2014, additional samples were run during the methanol treatment (see Sect. 2.7.3) for
511 the detection of benthic methanogens via qPCR. The qPCR results are shown in Fig. 7. For a better
512 comparison, the microbial abundances are plotted together with the sediment methane
513 concentrations from the methanol treatment, from which the rate calculation for the methanol-
514 methanogenesis at 0-1 cmbsf was done (shown in Fig. 5).

515 Methane concentrations increased over time revealing a slow increase in the first ~ 10 days, followed
516 by a steep increase between day 13 and day 20 and ending in a stationary phase.

517 A similar increase was seen in the abundance of total and methanogenic archaea. Total archaea
518 abundances increased sharply in the second week of the incubation reaching a maximum at day 16
519 ($\sim 5000 \cdot 10^6$ copies g^{-1}) and stayed around $3000 \cdot 10^6$ - $4000 \cdot 10^6$ copies g^{-1} over the course of the
520 incubation. Similarly, methanogenic archaea, namely the order *Methanosarcinales* and within this
521 order the family *Methanosarcinaceae*, showed a sharp increase in the first 2 weeks as well with the
522 highest abundances at day 16 ($\sim 6 \cdot 10^8$ copies g^{-1} and $\sim 1 \cdot 10^6$ copies g^{-1} , respectively). Until the end of
523 the incubation, the abundances of *Methanosarcinales* and *Methanosarcinaceae* decreased to about a
524 third of their maximum abundances ($\sim 2 \cdot 10^8$ copies g^{-1} and $\sim 0.4 \cdot 10^6$ copies g^{-1} , respectively).

525 3.6 Statistical Analysis

526 The PCA of integrated surface methanogenesis (0-5 cmbsf) (Fig.10) showed a strong positive
527 correlation with bottom water temperature (Fig. 9a), bottom water salinity (Fig. 9a), and surface
528 sediment POC content (Fig. 9c). Further, a positive correlation with bottom water methane and a
529 weak positive correlation with surface sediment C/N was detected (Fig. 9b). A strong negative
530 correlation was found with bottom water oxygen concentration (Fig. 9b). No correlation was found
531 with bottom water chlorophyll.

532 The PCA of methanogenesis depth profiles showed weak positive correlations with sediment depth
533 (Fig. 10a) and C/N (Fig. 10b), and showed negative correlations with POC (Fig. 10a).

534



535 4. Discussion

536 4.1 Methanogenesis in the sulfate-reducing zone

537 On the basis of the results presented in Fig. 1 and 2, it is evident that methanogenesis and sulfate
538 reduction were concurrently active in the surface sediments (0-30 cmbsf) at Boknis Eck. Even though
539 sulfate reduction rates were not measured directly, the decrease in sulfate concentrations with a
540 concomitant increase in sulfide within the upper 30 cmbsf indicate that sulfate reduction was active
541 (Fig. 1 and 2). Several earlier studies in Eckernförde Bay sediments confirmed the dominance of
542 sulfate reduction in the surface sediment, which revealed an activity of 100-10000 nmol cm⁻³ d⁻¹ in
543 the upper 25 cmbsf (Treude et al., 2005a; Bertics et al., 2013; Dale et al., 2013). Microbial
544 fermentation of organic matter was probably high in the organic-rich sediments of Eckernförde Bay
545 (POC contents of around 5 %, Fig. 1 and 2), providing high substrate availability and variety for
546 methanogenesis.

547

548 The results of this study further identified methylotrophy to be an important non-competitive
549 methanogenic pathway in the sulfate-reducing zone. The pathway utilizes alternative substrates,
550 such as methanol, to avoid competition with sulfate reducers for H₂ and acetate. The relevance of
551 methylotrophic methanogenesis in the sulfate-reducing zone was supported by the following
552 observations: 1) Hydrogenotrophic methanogenesis was up to two orders of magnitude lower than
553 net methanogenesis (Fig. 1 and 2), 2) methanogenesis increased when sulfate reduction was
554 inhibited (Fig. 5), 3) addition of BES did not result in the inhibition of methanogenesis (Fig. 6), 4)
555 addition of methanol increased potential methanogenesis rates up to three orders of magnitude (Fig.
556 6), 5) methylotrophic methanogens of the order *Methanosarcinales* were detected in the methanol-
557 treatment (Fig. 7), and 6) stable isotope probing revealed highly ¹³C-enriched methane produced
558 from ¹³C-labelled methanol (Fig. 6). In the following chapters, these arguments will be discussed in
559 more detail.

560 4.1.1 Hydrogenotrophic methanogenesis

561 We demonstrated that hydrogenotrophic methanogenesis was insufficient to explain the observed
562 net methanogenesis. The only exemption was March 2013, where rates of hydrogenotrophic
563 methanogenesis exceeded net methanogenesis in discrete depths (5-6 cmbsf and 25-30 cmbsf). It is
564 possible that additional carbon sources led to increased local fermentation processes, for instance
565 from the deposition of macro algae detritus, which is produced during winter storms and can be
566 transported into deeper sediment layers by bioturbation, where it is digested and released as fecal
567 pellets (Meyer-Reil, 1983; Bertics et al., 2013). Such additional carbon sources from fresh material
568 could lead to the local accumulation of excess hydrogen through fermentation and reduce the



569 competition for H₂ between sulfate reducers and methanogens (Treude et al., 2009). C/N ratios in
570 March 2013 were more scattered compared to other months in 2013 and 2014, indicating the
571 transport of labile material into the sediment. Eckernförde Bay sediments are known for bioturbation
572 especially during early spring by mollusks and polychaetes (D'Andrea et al., 1996; Orsi et al., 1996;
573 Bertics et al., 2013; Dale et al., 2013), and mollusk shells were observed even at depth of ~ 20 cmbsf
574 during sampling in the present study (personal observation).
575 Hydrogenotrophic methanogenesis was also detected in the gravity core in September 2013.
576 Maximum hydrogenotrophic rates were found at 45 cmbsf and 138 cmbsf, indicating a higher usage
577 of CO₂ and H₂ at depths > 40 cmbsf, where sulfate was depleted and thus the competition between
578 sulfate reducers and methanogens was relieved.

579 4.1.2 Inhibition of sulfate reducers

580 The competition between methanogens and sulfate reducers within the upper 30 cmbsf led to the
581 predominant utilization of non-competitive substrates by methanogenesis, as indicated by low
582 hydrogenotrophic methanogenesis rates (see discussion above). After the addition of the sulfate-
583 reducer inhibitor molybdate, competitive substrates (H₂/CO₂ and acetate (Oremland & Polcin, 1982;
584 King et al., 1983) were available for methanogenesis as indicated by the increase (up to 30 times) in
585 potential activity (Fig. 5 and 6). Notably, highest rates in the molybdate treatment were measured at
586 the shallowest sediment depth at most sampling months (except November 2013), pointing towards
587 the strongest competition between sulfate reducers and methanogens directly at the top 0-1 cmbsf,
588 which is confirmed by sulfate reduction maxima found at 0-1 cmbsf in earlier studies (Bertics et al.
589 2013; Treude et al. 2005).

590 4.1.3 Inhibition of methanogenesis by BES

591 Addition of BES did not result in the expected inhibition of potential methanogenesis; instead rates
592 were in the same range as the control treatment (Fig. 6). Either the inhibition of BES was incomplete,
593 or the methanogens were insensitive to BES (Hoehler et al., 1994; Smith & Mah, 1981; Santoro &
594 Konisky, 1987). However, the BES concentration used in the present study (60 mM) has been shown
595 to result in successful inhibition of methanogens in previous studies (Hoehler et al., 1994). Therefore,
596 the presence of methanogens that are insensitive BES was more likely. Insensitivity to BES would
597 support the hypothesis that methanogenesis in the sulfate reduction zone is mainly driven via the
598 methylotrophic pathway, as BES resistance was shown in *Methanosarcina* mutants in earlier studies
599 (Smith & Mah, 1981; Santoro & Konisky, 1987), a genus which we successfully detected in our
600 samples (for more details see Sect. 4.1.5), and which is known for mediating the methylotrophic
601 pathway (Keltjens & Vogels, 1993).



602 4.1.4 Methanol addition

603 High potential methanogenesis rates observed after the addition of the non-competitive substrate
604 methanol leads to the assumption that non-competitive substrates relieve the competition between
605 methanogens and sulfate reducers in surface sediments of Eckernförde Bay. Except for November
606 2013, highest rates in the methanol-treatment were detected in the upper 0-5 cmbsf and decreased
607 with depth (Fig. 5). Highest methanogenesis rates in the upper 0-5 cmbsf of the methanol-treatment
608 can be interpreted as follows: (1) The amount of non-competitive substrates including methanol was
609 most likely highest at the sediment surface, as those substrates are derived from fresh organic
610 matter, such as pectin or betaine and dimethylpropiothetin (both osmoprotectants) (Zinder, 1993).
611 (2) Sulfate reduction is most dominant in the 0-5 cmbsf (Treude et al., 2005a; Bertics et al., 2013),
612 which probably leads prevalent methanogens to be more adapted to the usage of non-competitive
613 substrates.

614 It should be noted that even though methanogenesis rates were calculated assuming a linear
615 increase in methane concentration over the entire incubation to make a better comparison between
616 different treatments, the methanol treatments generally showed a delayed response in methane
617 development (Supplement, Fig. S1). A similar delay was observed in organic-rich surface sediments
618 sampled off Peru and was explained by the predominant use of alternative non-competitive
619 substrates such as methylated sulfides (e.g. dimethyl sulfide or methanethiol (Maltby et al., 2016)). In
620 the marine environment, dimethyl sulfide mainly originates from the algae osmoregulatory compound
621 dimethylsulfoniopropionate (DMSP) (Van Der Maarel & Hansen, 1997), which could have
622 accumulated in Eckernförde Bay sediments, due to intense sedimentation of algae blooms (Bange et
623 al., 2011). Certain *Methanosarcina* species have been shown to use DMS as a substrate (Sieburth et
624 al., 1993; Van Der Maarel & Hansen, 1997), a genus, which has been detected in our samples (see
625 more details under Sect. 4.1.5).

626 Additionally, there are hints that methylated sulfur compounds may be generated through
627 nucleophilic attack by sulfide on the methyl groups in the sedimentary organic matter (Mitterer,
628 2010). As shown in the present study, sulfide was an abundant species in the surface sediment (up to
629 mM levels) (Fig. 1 and 2).

630 4.1.5 Presence of methylotrophic methanogens

631 Simultaneously with the increase in methane concentration after methanol addition in the surface
632 layer (0-1 cmbsf) in September 2014, the DNA counts for the order *Methanosarcinales* and the family
633 *Methanosarcinaceae* within the order *Methanosarcinales* increased 10² to 10⁶ times, respectively,
634 compared to the respective DNA abundances at the start of the incubation (Fig. 7). The successful
635 enrichment of *Methanosarcinaceae* indicates that this family is present in the natural environment
636 and thus could in part be responsible for the observed surface methanogenesis. As the members of



637 the family *Methanosarcinaceae* are known for utilization of methylated substrates (Boone et al.,
638 1993), our hypothesis for the predominant usage of non-competitive substrates is supported. The
639 delay in growth of *Methanosarcinales* and *Methanosarcinaceae*, however, also hints towards the
640 predominant usage of other non-competitive substrates besides methanol (see also Sect. 4.1.4).

641 4.1.6 Stable-isotope experiment

642 Samples taken in September 2014 for the labeling experiment (^{13}C -enriched methanol, initial isotopic
643 signature: +26 ‰) showed that methanol was completely consumed after 17 days and converted to
644 methane and CO_2 , as both revealed a concomitant enrichment in ^{13}C . The production of both
645 methane and CO_2 from methanol has been shown previously in different strains of methylotrophic
646 methanogens (Penger et al., 2012). As mentioned earlier, the major part of CO_2 was dissolved in the
647 porewater, which was not determined isotopically in this study, which is why we neglect the CO_2
648 development in the following.

649 Fractionation factors of methylotrophic methanogenesis from methanol to methane have been
650 found to be 1.07-1.08 (Heyer et al., 1976; Krzycki et al., 1987). This fractionation leads to a
651 progressive enrichment of ^{13}C in the residual methanol until all methanol is consumed. Accordingly,
652 methanol was enriched in ^{13}C in the first 13 days, as the consumption of ^{12}C -methanol was preferred
653 by the microbes. The fast conversion of methanol to methane can only be explained by the presence
654 of methylotrophic methanogens (e.g. members of the family *Methanosarcinaceae*, which is known
655 for the methylotrophic pathway (Keltjens & Vogels, 1993). Please note, however, that the storage of
656 the cores (3.5 months) prior to sampling could have led to shifts in the microbial community and thus
657 might not reflect in-situ conditions of the original microbial community in September 2014. The delay
658 in methane production also seen in the stable isotope experiment was, however, only slightly
659 different (methane developed earlier, between day 8 and 12, data not shown) from the non-labeled
660 methanol treatment (between day 10 to 16, Fig. S1), which leads us to the assumption that the
661 storage time at 1°C did not dramatically affect the methanogen community. Similar, in a previous
662 study with arctic sediments, addition of substrates had no stimulatory effect on the rate of
663 methanogenesis or on the methanogen community structure at low temperatures (5°C , (Blake et al.,
664 2015).

665 4.2 Environmental control of surface methanogenesis

666 Surface methanogenesis in Eckernförde Bay sediments showed variations throughout the sampling
667 period, which may be influenced by variable environmental factors such as temperature, salinity,
668 oxygen, and organic carbon. In the following, we will discuss the potential impact of those factors on
669 the magnitude and distribution of surface methanogenesis.

670 4.2.1 Temperature



671 During the sampling period, bottom water temperatures increased over the course of the year from
672 late winter (March, 3–4 °C) to autumn (November, 12°C, Fig. 1 and 2). The PCA revealed a strong
673 positive correlation between bottom water temperature and integrated surface methanogenesis (0–5
674 cmbsf). A temperature experiment conducted with sediment from ~75 cmbsf in September 2014
675 within a parallel study revealed a mesophilic temperature optimum of methanogenesis (20 °C, data
676 not shown). Whether methanogenesis in surface sediments (0–30 cm) has the same physiology
677 remains speculative. However, AOM organisms, which are closely related to methanogens (Knittel &
678 Boetius, 2009), studied in surface sediments from the same site were confirmed to have a mesophilic
679 physiology, too (Treude et al. 2005).

680

681 **4.2.2 Salinity and oxygen**

682 From March 2013 to November 2013, and from March 2014 to September 2014, salinity increased in
683 the bottom-near water (25 m) from 19 to 23 PSU and from 22 to 25 PSU (Fig. 1 and 2), respectively,
684 due the pronounced summer stratification in the water column between saline North Sea water and
685 less saline Baltic Sea water (Bange et al., 2011). The PCA detected a strong positive correlation
686 between integrated surface methanogenesis (0–5 cmbsf) and salinity in the bottom-near water (Fig.
687 9a). This correlation can hardly be explained by salinity alone, as methanogens feature a broad
688 salinity range from freshwater to hypersaline (Zinder, 1993). Even more, methanogenesis often
689 decreases with increasing salinity (Pattnaik et al., 2000), due to the concurrent increase of sulfate,
690 enabling sulfate-reducing bacteria to degrade organic matter prior to hydrogenotrophic and
691 acetoclastic methanogens (Oremland & Polcin, 1982). In fact, we found steep sulfate and sulfide
692 profiles at times of high salinity, indicating the presence of extensive sulfate reduction activity at the
693 sediment-water interface (Fig. 1 and 2). We therefore interpret positive correlation of
694 methanogenesis with salinity as an indirect indicator for a positive correlation with water column
695 stratification and hypoxia development. Accordingly, the PCA revealed a strong negative correlation
696 between oxygen concentration close to the seafloor and surface methanogenesis. In September
697 2014 bottom water levels probably reached zero levels as sulfide was detected in the bottom-near
698 water (25 m) 6 days after our sampling (H. Bange, pers. comm.). Hypoxia or anoxia in the bottom-
699 near water and the correlated absence of bioturbating and bioirrigating macrofauna (Dale et al.,
700 2013; Bertics et al., 2013) likely increased the habitable zone of methanogens close to the sediment-
701 water interface. Oxygen is an important factor controlling methanogenesis, as benthic methane is
702 mostly produced under strictly anoxic, highly reducing (< -200 mV) conditions (Oremland, 1988;
703 Zinder, 1993).

704

705 **4.2.4 Particulate organic carbon**



706 The supply of particulate organic carbon (POC) is one of the most important factors controlling
707 benthic heterotrophic processes, as it determines substrate availability and variety (Jørgensen,
708 2006). In Eckernförde Bay, the organic material reaching the sediment floor originates mainly from
709 phytoplankton blooms in spring, summer and autumn (Bange et al., 2011). It has been estimated that
710 > 50 % in spring (February/March), > 25 % in summer (July/August) and > 75 % in autumn
711 (September/October) of these blooms is reaching the seafloor (Smetacek et al., 1984), resulting in a
712 overall high organic carbon content of the sediment (5 wt %), which leads to high benthic microbial
713 degradation rates including sulfate reduction and methanogenesis (Whiticar, 2002; Treude et al.,
714 2005a; Bertics et al., 2013). Previous studies revealed that high organic matter availability can relieve
715 competition between sulfate reducers and methanogens in sulfate-containing, marine sediments
716 (Oremland et al., 1982; Holmer & Kristensen, 1994; Treude et al., 2009; Maltby et al., 2016).
717 To determine the effect of POC concentration and C/N ratio (as a negative indicator for the freshness
718 of POC) on surface methanogenesis, two PCAs were conducted with a) the focus on the upper 0-5
719 cmbsf, which is directly influenced by freshly sedimented organic material from the water column
720 (Fig. 9), and b) the focus on the depth profiles throughout the sediment cores (up to 30 cmbsf) (Fig.
721 10).

722 For the upper 0-5 cmbsf in the sediment, a strong positive correlation was found between surface
723 methanogenesis (integrated) and POC content (averaged) (Fig. 9c), indicating that POC content is an
724 important controlling factor for methanogenesis in this layer. In support, highest bottom-near water
725 chlorophyll concentrations coincided with highest bottom-near water methane concentrations and
726 high integrated surface methanogenesis (0-5 cmbsf) in September 2013, probably as a result of the
727 sedimentation of the summer phytoplankton bloom (Fig. 8). Indeed, the PCA revealed a strong
728 positive correlation between integrated surface methanogenesis rates and bottom-near water
729 methane concentrations (Fig. 9b) viewed over all investigated months. However, no correlation was
730 found between bottom water chlorophyll and integrated surface methanogenesis rates (Fig. 9). As
731 seen in Fig. 8, bottom-near high chlorophyll concentrations did not coincide with high bottom-near
732 methane concentration in June/September 2014. We explain this result by a time lag between
733 primary production in the water column and the export of the produced organic material to the
734 seafloor, which was probably even more delayed during stratification. Such a delay was observed in a
735 previous study (Bange et al., 2010), revealing enhanced water methane concentration close to the
736 seafloor approximately one month after the chlorophyll maximum. The C/N ratio (averaged over 0-5
737 cmbsf) showed a weak positive correlation with integrated surface methanogenesis (0-5 cmbsf),
738 which is surprising as we expected that a higher C/N ratio, indicative for less labile organic carbon,
739 should have a negative effect on non-competitive methanogenesis. However, methanogens are not
740 able to directly use most of the labile organic matter due their inability to process large molecules



741 (more than two C-C bondings) (Zinder, 1993). Methanogens are dependent on other microbial
742 groups to degrade large organic compounds (e.g. amino acids) for them (Zinder, 1993). Because of
743 this substrate speciation and dependence, a delay between the sedimentation of fresh, labile organic
744 matter and the increase in methanogenesis can be expected, which would not be captured by the
745 applied PCA.

746 In the PCA for the surface sediment profiles (0-30 cmbsf), POC showed a negative correlation with
747 methanogenesis, and sediment depth and C/N ratio showed a weak positive correlation with
748 methanogenesis (Fig 10.), which was also seen previously in the weak positive correlation between
749 integrated surface methanogenesis (0-5 cmbsf) and surface C/N (0-5 cmbsf). As POC, with the
750 exemption of the topmost sediment layer, remained basically unchanged over the top 30 cmbsf, its
751 negative correlation with methanogenesis is probably solely explained by the increase of
752 methanogenesis with sediment depth, and can therefore be excluded as a major controlling factor.
753 As sulfate in this zone was likely never depleted to levels that are critically limiting sulfate reduction
754 (lowest concentration 1300 μM , compare e.g. with Treude et al., 2014) we do not expect a significant
755 change in the competition between methanogens and sulfate reducers. It is therefore more likely
756 that the progressive degradation of organic matter into methanogenic substrates over depth and
757 time had a positive impact on methanogenesis. The C/N ratio indicates such a trend as the labile
758 fraction of POC decreased with depth. The mobilization of dissolved methanogenic substrates, such
759 as methanol, from organic matter would not be detectable by the C/N ratio as it is determined from
760 particulate samples.

761 4.3 Relevance of surface methanogenesis in Eckernförde Bay sediments

762 The time series station Boknis Eck in Eckernförde Bay is known for being a methane source to the
763 atmosphere throughout the year due to supersaturated waters, which result from significant benthic
764 methanogenesis and emission (Bange et al., 2010). The benthic methane formation is thought to take
765 place mainly in the deeper, sulfate-depleted sediment layers (Treude et al., 2005a; Whiticar, 2002).

766 In the present study, we show that surface methanogenesis within the sulfate zone is present despite
767 sulfate concentrations $> 1 \text{ mM}$, a limit above which methanogenesis has been thought to be
768 negligible (Alperin et al., 1994; Hoehler et al., 1994; Burdige, 2006), and thus could contribute to
769 benthic methane emissions. In support of this hypothesis, high dissolved methane concentration in
770 the water column occurred with concomitant high surface methanogenesis activity (Fig. 8).

771 In fact, surface methanogenesis in the Eckernförde Bay could even increase in the future, as
772 temperature and oxygen, two important controlling factors identified for surface methanogenesis
773 (Maltby et al., 2016) and this study), are predicted to increase and decrease, respectively (Lennartz et
774 al., 2014). We will therefore have a closer look at the magnitude and potential relevance of this
775 process for methane the benthic methane budget.



776 Surface methanogenesis rates determined in the present study are in a similar range of other sulfate-
777 containing, organic-rich surface sediments (e.g. salt marsh sediments, sediments from the upwelling
778 region off Chile and Peru, or coastal sediments from Limfjorden, North Sea), (Table 2, References
779 herein). In comparison with methanogenesis rates below the sulfate-methane- transition zone
780 (SMTZ) of organic-rich sediments (coastal and upwelling sediments), rates were mainly lower (2-5
781 times) (Table 2), which is explained by the competition relief below the SMTZ, which makes more
782 substrates available for methanogenesis.

783 We also performed a comparison between surface (0-30 cmbsf) and deep (below the SMTZ) net
784 methanogenesis for the present study site to investigate the relevance of surface methanogenesis in
785 Eckernförde Bay sediments for the overall benthic methane budget. In the gravity core of September
786 2013, the SMTZ was situated between 45 and 76 cmbsf (Fig. 3). The methane flux was estimated
787 according to Iversen & Jørgensen, (1993) using a sediment methane diffusion coefficient of $D_s =$
788 $1.64 \times 10^{-5} \text{ cm}^2 \text{ s}^{-1}$. The sediment diffusion coefficient was derived from the seawater methane-
789 diffusion coefficient at 10 °C (Schulz, 2006), which was corrected by porosity according to Iversen &
790 Jørgensen, (1993). The calculated deep methane production ($1.55 \text{ mmol m}^{-2} \text{ d}^{-1}$) was similar to earlier
791 calculated deep methanogenesis in Eckernförde Bay ($0.66 - 1.88 \text{ mmol m}^{-2} \text{ d}^{-1}$; Treude et al., 2005a).
792 However, integrated hydrogenotrophic methanogenesis measured in the presented study below 45
793 cmbsf (determined by interpolation, $0.5 \pm 0.2 \text{ mmol m}^{-2} \text{ d}^{-1}$) was up to 3 times lower compared to the
794 calculated deep methanogenesis, indicating that the interpolation missed hot spots of
795 hydrogenotrophic methanogenesis, as alternative pathways are not predicted for this zone given the
796 isotopic signature of methane (Whiticar, 2002). Surface methanogenesis in September 2013
797 represented 3-8 % of deep methanogenesis. While this percentage seems low, absolute surface
798 methanogenesis rates in Eckernförde Bay sediments are in the same magnitude as deep methane
799 production in other organic-rich sediments from the North Sea ($0.076 \text{ mmol m}^{-2} \text{ d}^{-1}$, Jørgensen &
800 Parkes, 2010), or from the upwelling region off Chile ($0.068-0.13 \text{ mmol m}^{-2} \text{ d}^{-1}$, Treude et al., 2005b),
801 indicating the general importance of this process. Compared to these other sites, Eckernförde Bay
802 features extremely high methanogenesis activity below the SMTZ, resulting in gas bubble formation
803 and ebullition (Abegg & Anderson, 1997; Jackson et al., 1998; Treude et al., 2005a).
804 How much of methane produced in the surface sediment is emitted into the water column depends
805 on the rate of methane consumption, i.e., aerobic and anaerobic oxidation of methane in the
806 sediment (Knittel & Boetius, 2009). In organic-rich sediments such as in the presented study, the oxic
807 sediment layer is often only mm-thick, due to the high rates of microbial organic matter degradation,
808 which rapidly consumes oxygen (Revsbech et al., 1980; Emerson et al., 1985; Jørgensen, 2006). Thus
809 the anaerobic oxidation of methane (AOM) might play a more dominant role in the present study. In
810 an earlier study from Eckernförde Bay, AOM rates were measured above the SMTZ (0-25 cmbsf), but



811 the authors concluded that it was fueled by deep methanogenesis (Treude et al., 2005a), as surface
812 integrated AOM rates ($0.8\text{-}1.5\text{ mmol m}^{-2}\text{ d}^{-1}$) were in the same magnitude as deep methane flux
813 ($0.66\text{-}1.88\text{ mmol m}^{-2}\text{ d}^{-1}$) from below the SMTZ (Treude et al., 2005a).
814 With the data set presented here we postulate that surface AOM above the SMTZ ($0.8\text{ mmol m}^{-2}\text{ d}^{-1}$,
815 Treude et al., (2005a) is mainly fueled by surface methanogenesis. If this is the case, then surface
816 methanogenesis is more likely in the range of $0.9\text{ mmol m}^{-2}\text{ d}^{-1}$ (AOM + net surface methanogenesis),
817 indicating that surface methanogenesis could play a much bigger role for benthic methane budgeting
818 than previously thought. Whether surface methanogenesis at Eckernförde Bay has the potential for
819 direct methane emissions into the water column goes beyond the informative nature of our dataset
820 and should be tested in future studies. Our study shows that surface methanogenesis correlates with
821 methane concentrations in the water column near the seafloor; however, so could also
822 methanogenesis and gas ebullition from below the SMTZ.

823 5. Summary

824 The present study demonstrated that methanogenesis and sulfate reduction were concurrently
825 active within the sulfate-reducing zone in sediments at Boknis Eck (Eckernförde Bay, SW Baltic Sea).
826 Observed methanogenesis was probably based on non-competitive substrates due to the
827 competition with sulfate reducers for the substrates H_2 and acetate. Accordingly, members of the
828 family *Methanosarcinaceae*, which are known for methylotrophic methanogenesis and were found in
829 the surface sediments, are likely to be responsible for the observed surface methanogenesis using
830 the substrates methanol, methylamines or methylated sulfides.
831 An important factor controlling surface methanogenesis in the upper 0-5 cmbsf was the POC content,
832 resulting in highest methanogenesis activity after summer and autumn phytoplankton blooms.
833 Increased stratification (indicated by increased salinity at the seafloor) was also found to be
834 beneficial for surface methanogenesis, as it leads the decline of oxygen below the pycnocline.
835 Accordingly, oxygen depletion during later summer showed a strong positive correlation with surface
836 methanogenesis, enabling more organic matter to reach the seafloor and providing a larger habitable
837 anoxic zone for methanogens in the surface sediment.
838 With increasing sediment depth (0-30 cmbsf), methanogenesis revealed only a positive correlation
839 with C/N ratio, indicating that a progressive mobilization of dissolved methanogenic substrates from
840 fermentation plays an important role for controlling non-competitive methanogenesis.
841 Even though surface methanogenesis was low compared to methanogenesis below the STTZ, it may
842 play an underestimated role in the methane budget at Boknis Eck, e.g., by directly fueling AOM
843 above the SMTZ.



844 **Author Contribution**

845 J.M. and T.T. designed the experiments. J.M. carried out all experiments. H.W. coordinated
846 measurements of water column methane and chlorophyll. C.L. and M.F. conducted molecular
847 analysis. M.S. coordinated ¹³C-Isotope measurements. J.M. prepared the manuscript with
848 contributions from all co-authors.

849 **Data Availability**

850 Research data for the present study can be accessed via the public data repository PANGEA
851 (doi:10.1594/PANGAEA.873185).

852 **Acknowledgements**

853 We thank the captain and crew of F.S. Alkor, F.K. Littorina and F.B. Polarfuchs for field assistance. We
854 thank G. Schüssler, F. Wulff, P. Wefers, A. Petersen, M. Lange, and F. Evers for field and laboratory
855 assistance. For the geochemical analysis we want to thank B. Domeyer, A. Bleyer, U. Lomnitz, R.
856 Suhrberg, and V. Thoenissen. We thank F. Malien, X. Ma, A. Kock and T. Baustian for the O₂, CH₄, and
857 chlorophyll measurements from the regular monthly Boknis Eck sampling cruises. Further we thank
858 R. Conrad and P. Claus at the MPI Marburg for the ¹³C-Methanol measurements. This study received
859 financial support through the Cluster of Excellence “The Future Ocean” funded by the German
860 Research Foundation, through the Sonderforschungsbereich (SFB) 754, and through a D-A-CH project
861 funded by the Swiss National Science Foundation and German Research foundation (grant no.
862 200021L_138057, 200020_159878/1). Further support was provided through the EU COST Action
863 PERGAMON (ESSEM 0902), through the BMBF project BioPara (grant no. 03SF0421B) and through
864 the EU’s H2020 program (Marie Curie grant NITROX # 704272 to CRL).

865

866 **References**

- 867 Abegg, F. & Anderson, A.L. (1997). The acoustic turbid layer in muddy sediments of Eckernförde Bay
868 , Western Baltic : methane concentration , saturation and bubble characteristics. *Marine*
869 *Geology*. 137. pp. 137–147.
- 870 Alperin, M.J., Albert, D.B. & Martens, C.S. (1994). Seasonal variations in production and consumption
871 rates of dissolved organic carbon in an organic-rich coastal sediment. *Geochimica et*
872 *Cosmochimica Acta*. 58 (22). pp. 4909–4930.
- 873 Bakker, D.E., Bange, H.W., Gruber, N., Johannessen, T., Upstill-Goddard, R.C., Borges, A.V., Delille, B.,
874 Löscher, C.R., Naqvi, S.W.A., Omar, A.M. & Santana-Casiano-J.M. (2014). Air-sea interactions of
875 natural long-lived greenhouse gases (CO₂, N₂O, CH₄) in a changing climate. In: P. S. Liss & M. T.
876 Johnson (eds.). *Ocean-Atmosphere Interactions of Gases and Particles*. Heidelberg: Springer-
877 Verlag, pp. 113–169.
- 878 Balzer, W., Pollehne, F. & Erlenkeuser, H. (1986). Cycling of Organic Carbon in a Marine Coastal
879 System. In: P. G. Sly (ed.). *Sediments and Water Interactions*. New York, NY: Springer New York,



- 880 pp. 325–330.
- 881 Bange, H.W., Bartell, U.H., Rapsomanikis, S. & Andreae, M.O. (1994). Methane in the Baltic and North
 882 Seas and a reassessment of the marine emissions of methane. *Global Biogeochemical Cycles*. 8
 883 (4). pp. 465–480.
- 884 Bange, H.W., Bergmann, K., Hansen, H.P., Kock, A., Koppe, R., Malien, F. & Ostrau, C. (2010).
 885 Dissolved methane during hypoxic events at the Boknis Eck time series station (Eckernförde
 886 Bay , SW Baltic Sea). *Biogeosciences*. 7. pp. 1279–1284.
- 887 Bange, H.W., Hansen, H.P., Malien, F., Laß, K., Karstensen, J., Petereit, C., Friedrichs, G. & Dale, A.
 888 (2011). Boknis Eck Time Series Station (SW Baltic Sea): Measurements from 1957 to 2010.
 889 *LOICZ-Affiliated Activities*. Inprint 20. pp. 16–22.
- 890 Bertics, V.J., Löscher, C.R., Salonen, I., Dale, A.W., Gier, J., Schmitz, R.A. & Treude, T. (2013).
 891 Occurrence of benthic microbial nitrogen fixation coupled to sulfate reduction in the seasonally
 892 hypoxic Eckernförde Bay, Baltic Sea. *Biogeosciences*. 10 (3). pp. 1243–1258.
- 893 Blake, L.I., Tveit, A., Øvreås, L., Head, I.M. & Gray, N.D. (2015). *Response of Methanogens in Arctic*
 894 *Sediments to Temperature and Methanogenic Substrate Availability*.
- 895 Buckley, D.H., Baumgartner, L.K. & Visscher, P.T. (2008). Vertical distribution of methane metabolism
 896 in microbial mats of the Great Sippewissett Salt Marsh. *Environmental microbiology*. 10 (4). pp.
 897 967–77.
- 898 Burdige, D.J. (2006). *Geochemistry of Marine Sediments*. New Jersey, U.S.A.: Princeton University
 899 Press.
- 900 Cicerone, R.J. & Oremland, R.S. (1988). Biogeochemical aspects of atmospheric methane. *Global*
 901 *Biogeochemical Cycles*. 2 (4). pp. 299–327.
- 902 Crill, P.M. & Martens, C.S. (1986). Methane production from bicarbonate and acetate in an anoxic
 903 marine sediment. *Geochimica et Cosmochimica Acta*. 50. pp. 2089–2097.
- 904 D’Andrea, a. F., Craig, N.I. & Lopez, G.R. (1996). Benthic macrofauna and depth of bioturbation in
 905 Eckernförde Bay, southwestern Baltic Sea. *Geo-Marine Letters*. 16 (3). pp. 155–159.
- 906 Dale, a. W., Bertics, V.J., Treude, T., Sommer, S. & Wallmann, K. (2013). Modeling benthic–pelagic
 907 nutrient exchange processes and porewater distributions in a seasonally hypoxic sediment:
 908 evidence for massive phosphate release by Beggiatoa? *Biogeosciences*. 10 (2). pp. 629–651.
- 909 Denman, K.L., Brasseur, G., Chidthaisong, A., Ciais, P., Cox, P.M., Dickinson, R.E., Hauglustaine, D.,
 910 Heinze, C., Holland, E., Jacob, D., Lohmann, U., Ramachandran, S., da Silva Dias, P.L., Wofsy, S.C.
 911 & Zhang, X. (2007). Couplings Between Changes in the Climate System and Biogeochemistry. In:
 912 S. Solomon, D. Qin, M. Manning, Z. Chen, M. Marquis, K. B. Averyt, M. Tignor, & H. L. Miller
 913 (eds.). *Climate Change 2007: The Physical Science Basis. Contribution of Working Group I to the*
 914 *Fourth Assessment Report of the Intergovernmental Panel on Climate Change*. Cambridge,
 915 United Kingdom and New York, NY, USA: Cambridge University Press.
- 916 Emerson, S., Fischer, K., Reimers, C. & Heggge, D. (1985). Organic carbon dynamics and preservation
 917 in deep-sea sediments. *Deep Sea Research Part A. Oceanographic Research Papers*. 32 (1). pp.
 918 1–21.
- 919 EPA (2010). *Methane and nitrous oxide emissions from natural sources*. Washington, DC, USA.
- 920 Ferdelman, T.G., Lee, C., Pantoja, S., Harder, J., Bebout, B.M. & Fossing, H. (1997). Sulfate reduction
 921 and methanogenesis in a Thioploca-dominated sediment off the coast of Chile. *Geochimica et*
 922 *Cosmochimica Acta*. 61 (15). pp. 3065–3079.
- 923 Gier, J., Sommer, S., Löscher, C.R., Dale, A.W., Schmitz, R.A. & Treude, T. (2016). Nitrogen fixation in
 924 sediments along a depth transect through the Peruvian oxygen minimum zone. *Biogeosciences*.
 925 13 (14). pp. 4065–4080.



- 926 Grasshoff, K., Ehrhardt, M. & Kremmling, K. (1999). *Methods of Seawater Analysis*. Weinheim: Verlag
 927 Chemie.
- 928 Hansen, H.-P., Giesenhausen, H.C. & Behrends, G. (1999). Seasonal and long-term control of bottom-
 929 water oxygen deficiency in a stratified shallow-water coastal system. *ICES Journal of Marine*
 930 *Science*. 56. pp. 65–71.
- 931 Hartmann, D.L., Klein Tank, A.M.G., Rusticucci, M., Alexander, L.V., Brönnimann, S., Charabi, Y.,
 932 Dentener, F.J., Dlugokencky, D.R., Easterling, D.R., Kaplan, A., Soden, B.J., Thorne, P.W., Wild,
 933 M. & Zhai, P.M. (2013). Observations: Atmosphere and Surface. In: *Climate Change 2013: The*
 934 *pHysical Science Basis. Contribution Group I to the Fifth Assessment Report of the*
 935 *Intergovernmental Panel on Climate Change*. United Kingdom and New York, NY, USA:
 936 Cambridge University Press.
- 937 Heyer, J., Hübner, H. & Maaß, I. (1976). Isotopenfraktionierung des Kohlenstoffs bei der mikrobiellen
 938 Methanbildung. *Isotopenpraxis Isotopes in Environmental and Health Studies*. [Online]. 12 (5).
 939 pp. 202–205. Available from:
 940 <http://www.tandfonline.com/doi/abs/10.1080/10256017608543912>. [Accessed: 15 October
 941 2014].
- 942 Hoehler, T.M., Alperin, M.J., Albert, D.B. & Martens, C.S. (1994). Field and laboratory studies of
 943 methane oxidation in an anoxic marine sediment: Evidence for a methanogen-sulfate reducer
 944 consortium. *Global Biogeochemical Cycles*. 8 (4). pp. 451–463.
- 945 Holmer, M. & Kristensen, E. (1994). Coexistence of sulfate reduction and methane production in an
 946 organic-rich sediment. *Marine Ecology Progress Series*. 107. pp. 177–184.
- 947 Iversen, N. & Jørgensen, B.B. (1993). Diffusion coefficients of sulfate and methane in marine
 948 sediments: Influence of porosity. *Geochimica et Cosmochimica Acta*. 57 (3). pp. 571–578.
- 949 Jackson, D.R., Williams, K.L., Wever, T.F., Friedrichs, C.T. & Wright, L.D. (1998). Sonar evidence for
 950 methane ebullition in Eckernförde Bay. *Continental Shelf Research*. 18. pp. 1893–1915.
- 951 Jørgensen, B.B. (2006). Bacteria and marine Biogeochemistry. In: H. D. Schulz & M. Zabel (eds.).
 952 *Marine Geochemistry*. Berlin/Heidelberg: Springer-Verlag, pp. 173–207.
- 953 Jørgensen, B.B. & Parkes, R.J. (2010). Role of sulfate reduction and methane production by organic
 954 carbon degradation in eutrophic fjord sediments (Limfjorden, Denmark). *Limnology and*
 955 *Oceanography*. 55 (3). pp. 1338–1352.
- 956 Keltjens, J.T. & Vogels, G.D. (1993). Conversion of methanol and methylamines to methane and
 957 carbon dioxide. In: J. G. Ferry (ed.). *Methanogenesis: Ecology, Physiology, Biochemistry &*
 958 *Genetics*. Chapman & Hall, pp. 253–303.
- 959 King, G.M., Klug, M.J. & Lovley, D.R. (1983). Metabolism of acetate, methanol, and methylated
 960 amines in intertidal sediments of lowes cove, maine. *Applied and environmental microbiology*.
 961 45 (6). pp. 1848–1853.
- 962 Knittel, K. & Boetius, A. (2009). Anaerobic oxidation of methane: progress with an unknown process.
 963 *Annual review of microbiology*. 63. pp. 311–34.
- 964 Krzycki, J.A., Kenealy, W.R., Deniro, M.J. & Zeikus, J.G. (1987). Stable Carbon Isotope Fractionation by
 965 *Methanosarcina barkeri* during Methanogenesis from Acetate, Methanol, or Carbon Dioxide-
 966 Hydrogen. *Applied and environmental microbiology*. 53 (10).
- 967 Kuivila, K.M., Murray, J.W. & Devol, a. H. (1990). Methane production in the sulfate-depleted
 968 sediments of two marine basins. *Geochimica et Cosmochimica Acta*. 54. pp. 403–411.
- 969 Lennartz, S.T., Lehmann, A., Herrford, J., Malien, F., Hansen, H.-P., Biester, H. & Bange, H.W. (2014).
 970 Long-term trends at the Boknis Eck time series station (Baltic Sea), 1957–2013: does climate
 971 change counteract the decline in eutrophication? *Biogeosciences*. 11 (22). pp. 6323–6339.



- 972 Van Der Maarel, M.J.E.C. & Hansen, T. a. (1997). Dimethylsulfoniopropionate in anoxic intertidal
 973 sediments: A precursor of methanogenesis via dimethyl sulfide, methanethiol, and
 974 methiolpropionate. *Marine Geology*. 137 (1–2). pp. 5–12.
- 975 Maltby, J., Sommer, S., Dale, A.W. & Treude, T. (2016). Microbial methanogenesis in the sulfate-
 976 reducing zone of surface sediments traversing the Peruvian margin. *Biogeosciences*. 13. pp.
 977 283–299.
- 978 Martens, C.S., Albert, D.B. & Alperin, M.J. (1998). Biogeochemical processes controlling methane in
 979 gassy coastal sediments---Part 1 . A model coupling organic matter flux to gas production ,
 980 oxidation and transport. *Continental Shelf Research*. 18. pp. 14–15.
- 981 Meyer-Reil, L.-A. (1983). Benthic response to sedimentation events during autumn to spring at a
 982 shallow water station in the Western Kiel Bight. *Marine Biology*. 77. pp. 247–256.
- 983 Mitterer, R.M. (2010). Methanogenesis and sulfate reduction in marine sediments: A new model.
 984 *Earth and Planetary Science Letters*. 295 (3–4). pp. 358–366.
- 985 Naqvi, S.W. a., Bange, H.W., Farías, L., Monteiro, P.M.S., Scranton, M.I. & Zhang, J. (2010). Marine
 986 hypoxia/anoxia as a source of CH₄ and N₂O. *Biogeosciences*. 7 (7). pp. 2159–2190.
- 987 Oremland, R.S. (1988). Biogeochemistry of methanogenic bacteria. In: A. J. B. Zehnder (ed.). *Biology*
 988 *of Anaerobic Microorganisms*. New York: J. Wiley & Sons, pp. 641–705.
- 989 Oremland, R.S. & Capone, D.G. (1988). Use of specific inhibitors in biogeochemistry and microbial
 990 ecology. In: K. C. Marshall (ed.). *Advances in Microbial Ecology*. Advances in Microbial Ecology.
 991 Boston, MA: Springer US, pp. 285–383.
- 992 Oremland, R.S., Marsh, L.M. & Polcin, S. (1982). Methane production and simultaneous sulfate
 993 reduction in anoxic, salt-marsh sediments. *Nature*. 286. pp. 143–145.
- 994 Oremland, R.S. & Polcin, S. (1982). Methanogenesis and Sulfate Reduction : Competitive and
 995 Noncompetitive Substrates in Estuarine Sediments. *Applied and Environmental Microbiology*. 44
 996 (6). pp. 1270–1276.
- 997 Orsi, T.H., Werner, F., Milkert, D., Anderson, a. L. & Bryant, W.R. (1996). Environmental overview of
 998 Eckernförde Bay, northern Germany. *Geo-Marine Letters*. 16 (3). pp. 140–147.
- 999 Pattnaik, P., Mishra, S.R., Bharati, K., Mohanty, S.R., Sethunathan, N. & Adhya, T.K. (2000). Influence
 1000 of salinity on methanogenesis and associated microflora in tropical rice soils. *Microbiological*
 1001 *research*. [Online]. 155 (3). pp. 215–220. Available from: [http://dx.doi.org/10.1016/S0944-](http://dx.doi.org/10.1016/S0944-5013(00)80035-X)
 1002 [5013\(00\)80035-X](http://dx.doi.org/10.1016/S0944-5013(00)80035-X).
- 1003 Penger, J., Conrad, R. & Blaser, M. (2012). Stable carbon isotope fractionation by methylotrophic
 1004 methanogenic archaea. *Applied and environmental microbiology*. [Online]. 78 (21). pp. 7596–
 1005 602. Available from:
 1006 <http://www.pubmedcentral.nih.gov/articlerender.fcgi?artid=3485729&tool=pmcentrez&render>
 1007 [type=abstract](http://www.pubmedcentral.nih.gov/articlerender.fcgi?artid=3485729&tool=pmcentrez&render). [Accessed: 13 October 2014].
- 1008 Pimenov, N., Davidova, I., Belyaev, S., Lein, A. & Ivanov, M. (1993). Microbiological processes in
 1009 marine sediments in the Zaire River Delta and the Benguela upwelling region. *Geomicrobiology*
 1010 *Journal*. 11 (3–4). pp. 157–174.
- 1011 Preisler, A., de Beer, D., Lichtschlag, A., Lavik, G., Boetius, A. & Jørgensen, B.B. (2007). Biological and
 1012 chemical sulfide oxidation in a Beggiatoa inhabited marine sediment. *The ISME journal*. 1 (4).
 1013 pp. 341–353.
- 1014 Reeburgh, W. (2007). Oceanic methane biogeochemistry. *Chemical Reviews*. pp. 486–513.
- 1015 Revsbech, N.P., Jørgensen, B.B. & Blackburn, T.H. (1980). Oxygen in the sea bottom measured with a
 1016 microelectrode. *Science*. 207 (4437). pp. 1355–1356.
- 1017 Santoro, N. & Konisky, J. (1987). Characterization of bromoethanesulfonate-resistant mutants of



- 1018 Methanococcus voltae: Evidence of a coenzyme M transport system. *Journal of Bacteriology*.
 1019 169 (2). pp. 660–665.
- 1020 Schlüter, M., Sauter, E., Hansen, H.-P. & Suess, E. (2000). Seasonal variations of bioirrigation in
 1021 coastal sediments: modelling of field data. *Geochimica et Cosmochimica Acta*. 64 (5). pp. 821–
 1022 834.
- 1023 Schulz, H.D. (2006). Quantification of early diagenesis: dissolved constituents in marine pore water.
 1024 In: H. D. Schulz & M. Zabel (eds.). *Marine Geochemistry*. Berlin, Heidelberg: Springer Berlin
 1025 Heidelberg, pp. 75–124.
- 1026 Seeberg-Elverfeldt, J., Schluter, M., Feseker, T. & Kolling, M. (2005). Rhizon sampling of porewaters
 1027 near the sediment-water interface of aquatic systems. *Limnology and Oceanography-Methods*.
 1028 3. pp. 361–371.
- 1029 Senior, E., Lindström, E.B., Banat, I.M. & Nedwell, D.B. (1982). Sulfate reduction and methanogenesis
 1030 in the sediment of a saltmarsh on the East coast of the United kingdom. *Applied and
 1031 environmental microbiology*. 43 (5). pp. 987–996.
- 1032 Sieburth, J.M., Johnson, P.W., Macario, a. J.L. & De Macario, E.C. (1993). C1 bacteria in the water
 1033 column of Chesapeake Bay, USA. II. The dominant O₂- and H₂S-tolerant methylotrophic
 1034 methanogens, coenriched with their oxidative and sulphate reducing bacterial consorts, are all
 1035 new immunotypes and probably include new taxa. *Marine Ecology Progress Series*. 95 (1–2). pp.
 1036 81–89.
- 1037 Smetacek, V. (1985). The Annual Cycle of Kiel Bight Plankton: A Long-Term Analysis. *Estuaries*. 8
 1038 (June). pp. 145–157.
- 1039 Smetacek, V., von Bodungen, B., Knoppers, B., Peinert, R., Pollehne, F., Stegmann, P. & Zeitzschel, B.
 1040 (1984). Seasonal stages characterizing the annual cycle of an inshore pelagic system. *Rapports
 1041 et Proces-Verbaux des Reunions Conseil International pour l'Exploration de la Mer*. 186. pp.
 1042 126–135.
- 1043 Smith, M.R. & Mah, R. a. (1981). 2-Bromoethanesulfonate: A selective agent for isolating
 1044 resistant Methanosarcina mutants. *Current Microbiology*. 6 (5). pp. 321–326.
- 1045 Thießen, O., Schmidt, M., Theilen, F., Schmitt, M. & Klein, G. (2006). Methane formation and
 1046 distribution of acoustic turbidity in organic-rich surface sediments in the Arkona Basin, Baltic
 1047 Sea. *Continental Shelf Research*. 26 (19). pp. 2469–2483.
- 1048 Treude, T., Krause, S., Maltby, J., Dale, A.W., Coffin, R. & Hamdan, L.J. (2014). Sulfate reduction and
 1049 methane oxidation activity below the sulfate-methane transition zone in Alaskan Beaufort Sea
 1050 continental margin sediments: Implications for deep sulfur cycling. *Geochimica et
 1051 Cosmochimica Acta*. 144. pp. 217–237.
- 1052 Treude, T., Krüger, M., Boetius, A. & Jørgensen, B.B. (2005a). Environmental control on anaerobic
 1053 oxidation of methane in the gassy sediments of Eckernförde Bay (German Baltic). *Limnology
 1054 and Oceanography*. 50 (6). pp. 1771–1786.
- 1055 Treude, T., Niggemann, J., Kallmeyer, J., Wintersteller, P., Schubert, C.J., Boetius, A. & Jørgensen, B.B.
 1056 (2005b). Anaerobic oxidation of methane and sulfate reduction along the Chilean continental
 1057 margin. *Geochimica et Cosmochimica Acta*. 69 (11). pp. 2767–2779.
- 1058 Treude, T., Smith, C.R., Wenzhöfer, F., Carney, E., Bernardino, A.F., Hannides, A.K., Krgüer, M. &
 1059 Boetius, A. (2009). Biogeochemistry of a deep-sea whale fall: Sulfate reduction, sulfide efflux
 1060 and methanogenesis. *Marine Ecology Progress Series*. 382. pp. 1–21.
- 1061 Welschmeyer, N.A. (1994). Fluorometric analysis of chlorophyll a in the presence of chlorophyll b and
 1062 pheopigments. *Limnology and Oceanography*. 39 (8). pp. 1985–1992.
- 1063 Wever, T.F., Abegg, F., Fiedler, H.M., Fechner, G. & Stender, I.H. (1998). Shallow gas in the muddy
 1064 sediments of Eckernförde Bay, Germany. *Continental Shelf Research*. 18. pp. 1715–1739.



- 1065 Wever, T.F. & Fiedler, H.M. (1995). Variability of acoustic turbidity in Eckernförde Bay (southwest
1066 Baltic Sea) related to the annual temperature cycle. *Marine Geology*. 125. pp. 21–27.
- 1067 Whiticar, M.J. (2002). Diagenetic relationships of methanogenesis, nutrients, acoustic turbidity,
1068 pockmarks and freshwater seepages in Eckernförde Bay. *Marine Geology*. 182. pp. 29–53.
- 1069 Widdel, F. & Bak, F. (1992). Gram-Negative Mesophilic Sulfate-Reducing Bacteria. In: A. Balows, H. G.
1070 Trüper, M. Dworkin, W. Harder, & K.-H. Schleifer (eds.). *The Prokaryotes*. New York, NY:
1071 Springer New York, pp. 3352–3378.
- 1072 Wuebbles, D.J. & Hayhoe, K. (2002). Atmospheric methane and global change. *Earth-Science Reviews*.
1073 57 (3–4). pp. 177–210.
- 1074 Zinder, S.H. (1993). Physiological ecology of methanogens. In: J. G. Ferry (ed.). *Methanogenesis*. New
1075 York, NY: Chapman & Hall, pp. 128–206.
- 1076



1077 **Figure Captions**

1078 **Figure 1:** Parameters measured in the water column and sediment at each sampling month in the
1079 year 2013. Net methanogenesis (MG) and hydrogenotrophic (hydr.) methanogenesis rates are shown
1080 in triplicates with mean (solid line).

1081 **Figure 2:** Parameters measured in the water column and sediment at each sampling month in the
1082 year 2014. Net methanogenesis (MG) and hydrogenotrophic (hydr.) methanogenesis rates are shown
1083 in triplicates with mean (solid line).

1084 **Figure 3:** Parameters measured in the sediment in the gravity core in September 2013.
1085 Hydrogenotrophic (hydr.) methanogenesis rates are shown in triplicates with mean (solid line).

1086 **Figure 4:** Integrated net methanogenesis (MG) rates and hydrogenotrophic MG rates (0-25 cmbsf) for
1087 each time point.

1088 **Figure 5:** Potential methanogenesis rates of the four different treatments in November 2013, March
1089 2014, June 2014 and September 2014. Control (blue symbols) is describing the treatment with
1090 sediment plus artificial seawater containing natural salinity (24 PSU) and sulfate concentrations (17
1091 mM), molybdate (green symbols) is the treatment with addition of molybdate (22 mM), BES (purple
1092 symbols) is the treatment with 60 mM BES addition, and methanol (red symbols) is the treatment
1093 with addition of 10 mM methanol. Shown are triplicates per depth interval and the mean as a solid
1094 line. Please note the different x-axis for the methanol treatment (red).

1095 **Figure 6:** Concentrations (A) and isotope composition (B) of porewater methanol (CH₃OH), headspace
1096 methane (CH₄), and headspace carbon dioxide (CO₂) during the sediment-slurry experiment (with
1097 sediment from the 0-1 cmbsf horizon in September 2014) with addition of ¹³C-enriched methanol
1098 (¹³C:¹²C = 1:1000). Experiment was conducted over 37 days at in-situ temperature (13°C). Shown are
1099 means (from triplicates) with standard deviation.

1100 **Figure 7:** Sediment methane concentrations over time in the treatment with addition of methanol
1101 (10 mM) are shown above. Shown are triplicate values per measurement. DNA copies of *Archaea*,
1102 *Methanosarcinales* and *Methanosarcinaceae* are shown below in duplicates per measurement.
1103 Please note the secondary y-axis for *Methanosarcinales* and *Methanosarcinaceae*. More data are
1104 available for methane (determined in the gas headspace) than from DNA samples (taken from the
1105 sediment) as sample volume for molecular analyzes was limited.

1106 **Figure 8:** Temporal development of integrated net surface methanogenesis (0-5 cmbsf) in the
1107 sediment and chlorophyll (green) and methane concentrations (orange) in the bottom water (25 m).



1108 Methanogenesis (MG) rates and methane concentrations are shown in means (from triplicates) with
1109 standard deviation.

1110 **Figure 9:** Principle component analysis (PCA) from three different angles of integrated surface
1111 methanogenesis (0-5 cmbsf) and surface particulate organic carbon averaged over 0-5 cmbsf (surface
1112 sediment POC), surface C/N ratio averaged over 0-5 cmbsf (surface sediment C/N), bottom water
1113 salinity, bottom water temperature (T), bottom water methane (CH₄), bottom water oxygen (O₂), and
1114 bottom water chlorophyll. Data were transformed into ranks before analysis. a) Correlation biplot of
1115 principle components 1 and 2, b) correlation biplot of principle components 1 and 3, c) correlation
1116 biplot of principle components 2 and 3. Correlation biplots are shown in a multidimensional space
1117 with parameters shown as green lines and samples shown as black dots. Parameters pointing into
1118 the same direction are positively related; parameters pointing in the opposite direction are
1119 negatively related.

1120

1121 **Figure 10:** Principle component analysis (PCA) from two different angles of surface methanogenesis
1122 depth profiles and sampling month (Month), sediment depth, depth profiles of particulate organic
1123 carbon (POC) and C/N ratio (C/N). Data was transformed into ranks before analysis. a) Correlation
1124 biplot of principle components 1 and 2, b) correlation biplot of principle components 1 and 3.
1125 Correlation biplots are shown in a multidimensional space with parameters shown as green lines and
1126 samples shown as black dots. Parameters pointing into the same direction are positively related;
1127 parameters pointing in the opposite direction are negatively related.

1128

1129

1130

1131

1132

1133

1134



1135

1136 **Table 1:** Sampling months with bottom water (~ 2 m above seafloor) temperature (Temp.), dissolved
 1137 oxygen (O₂) and dissolved methane (CH₄) concentration

Sampling Month	Date	Instrument	Temp. (°C)	O ₂ (μM)	CH ₄ (nM)	Type of Analysis
March 2013	13.03.2013	CTD	3	340	30	WC
		MUC				All
Juni 2013	27.06.2013	CTD	6	94	125	WC
		MUC				All
September 2013	25.09.2013	CTD	10	bdl	262*	WC
		MUC				All
		GC				GC-All
November 2013	08.11.2013	CTD	12	163	13	WC
		MUC				All
March 2014	13.03.2014	CTD	4	209	41*	WC
		MUC				All
June 2014	08.06.2014	CTD	7	47	61	WC
		MUC				All
September 2014	17.09.2014	CTD	13	bdl	234	WC
		MUC				All

1138 MUC = multicorer, GC= gravity corer, CTD = CTD/Rosette, bdl= below detection limit (5μM), All = methane gas
 1139 analysis, porewater analysis, sediment geochemistry, net methanogenesis analysis, hydrogenotrophic
 1140 methanogenesis analysis, GC-All= analysis for gravity cores including methane gas analysis, porewater analysis,
 1141 sediment geochemistry, hydrogenotrophic methanogenesis analysis, WC= Water column analyses including
 1142 methane analysis, chlorophyll analysis

1143 **Concentrations from the regular monthly Boknis Eck sampling cruises on 24.09.13 and 05.03. 14 (www.bokniseck.de)

1144

1145

1146

1147

1148

1149

1150

1151



1152 **Table 2:** Comparison of surface methanogenesis rates in shallow water marine sediments of different
 1153 geographical origin

Study site	Water depth (m)	Sediment depths (cm)	Rate (nmol cm ⁻³ d ⁻¹)	Reference
<i>Sulfate-containing, organic-rich sediments</i>				
Eckernförde Bay (Baltic Sea)	28	0-25	0 -1.3	Present study
Upwelling region off Peru (Pacific)	70-1025	0-25	0-1.5	(Maltby et al., 2016)
Upwelling region off Chile (Pacific)	87	0-6	0-0.6	(Ferdelman et al., 1997)
Limfjorden (North Sea)	7-10	0-100	0-0.05	(Jørgensen & Parkes, 2010)
Colne Point Saltmarsh (Essex, UK)	-	0-30	0-0.03	(Senior et al., 1982)
<i>Sulfate-depleted, organic-rich sediments (sediment depth marks the depth at which sulfate was depleted)</i>				
Eckernförde Bay (Baltic Sea)	28	> 100	0.01-1.4	Present Study
Limfjorden (North Sea)	7-10	> 100	0.01-3.1	(Jørgensen & Parkes, 2010)
Saanich Inlet (British Columbia, Canada)	225	> 20	0.3-7.0	(Kuivila et al., 1990)
Upwelling region off Peru (Pacific)	78	> 50	0-2.1	(Maltby et al., 2016)

1154

1155

1156

1157

1158

1159

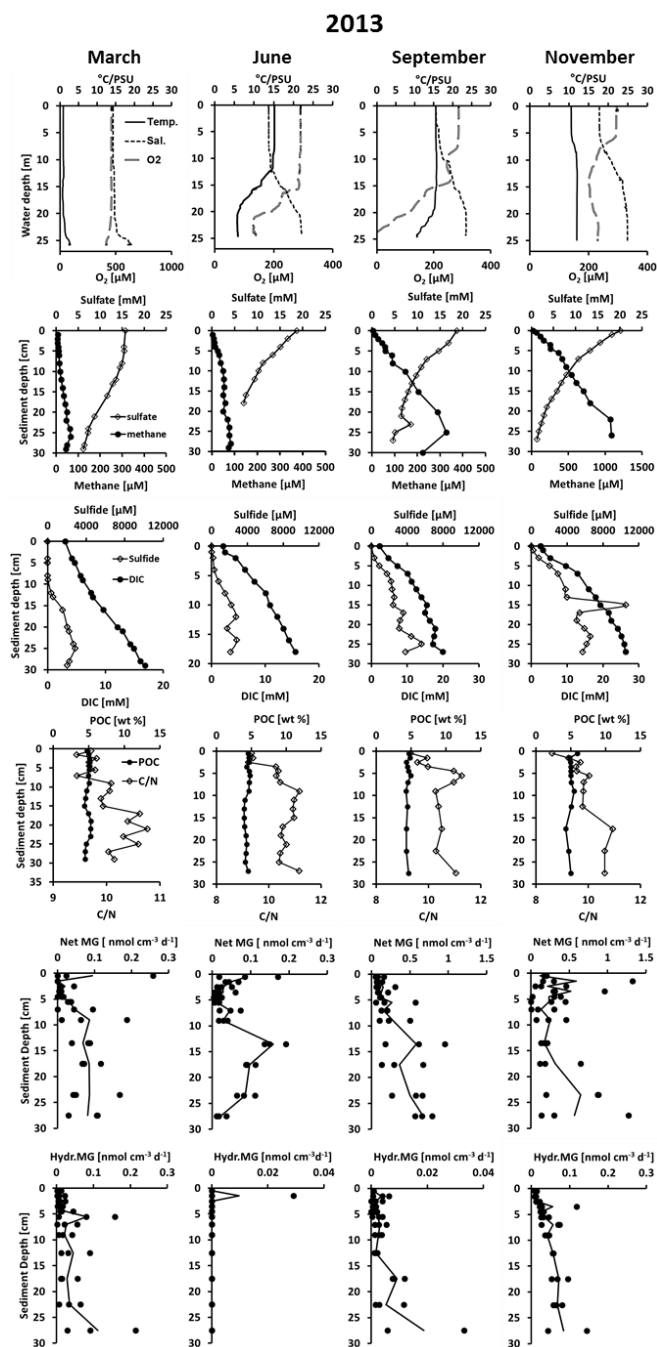
1160

1161



1162 Figures

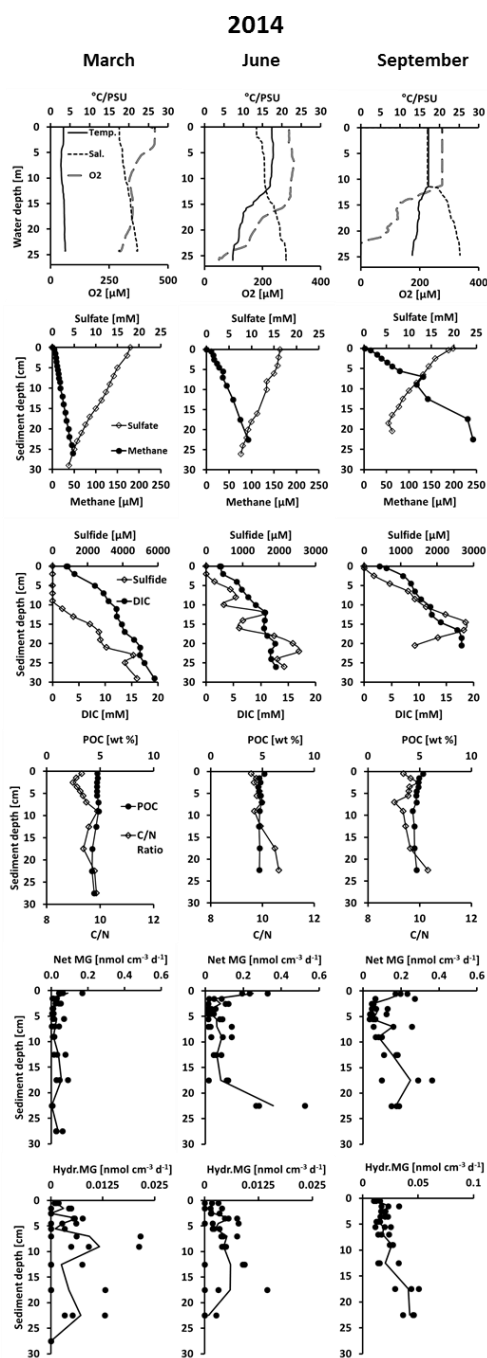
1163 Figure 1



1164



1165 **Figure 2**



1166

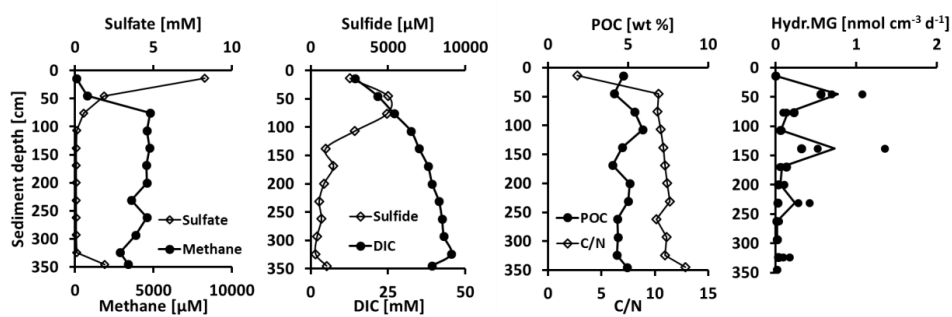
1167



1168

1169 **Figure 3**

1170



1171

1172

1173

1174

1175

1176

1177

1178

1179

1180

1181

1182

1183

1184

1185

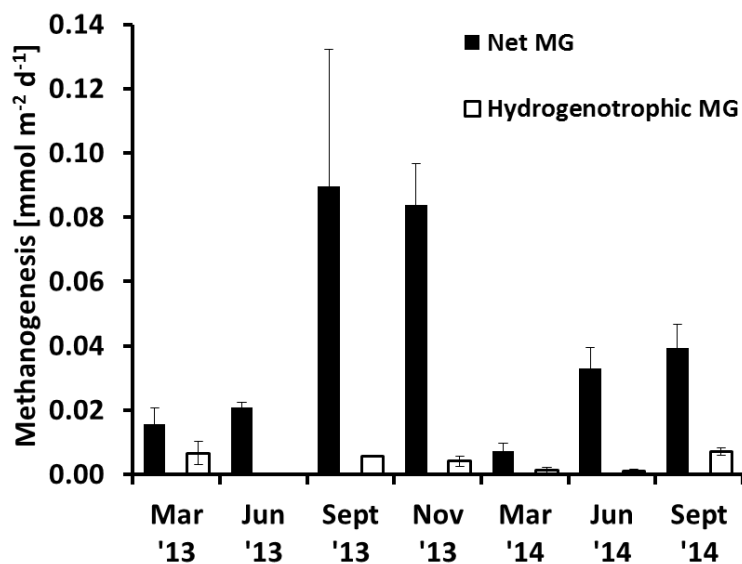
1186



1187

1188 **Figure 4**

1189



1190

1191

1192

1193

1194

1195

1196

1197

1198

1199

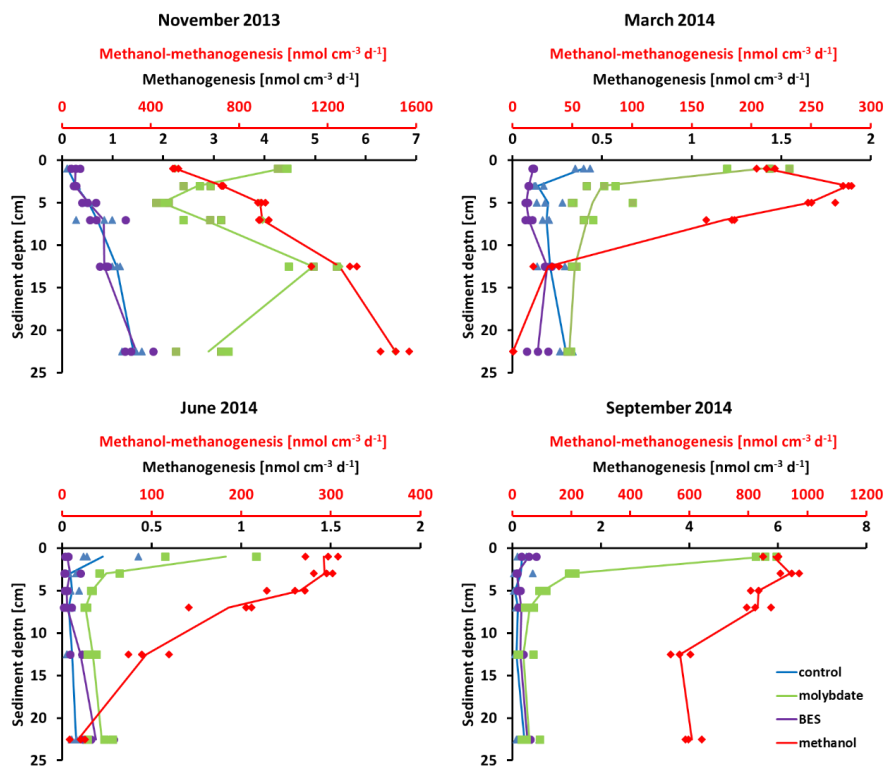
1200

1201



1202 **Figure 5**

1203



1204

1205

1206

1207

1208

1209

1210

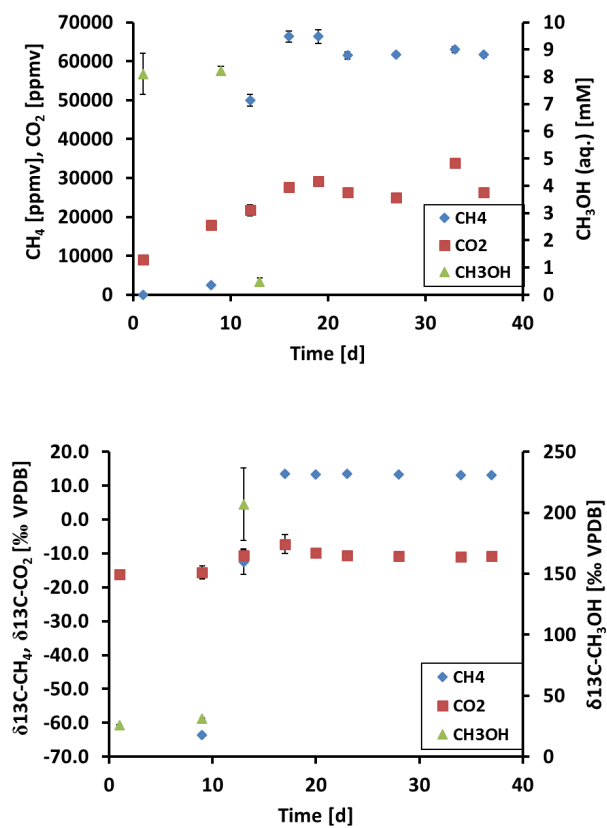
1211

1212

1213



1214 Figure 6



1215

1216

1217

1218

1219

1220

1221

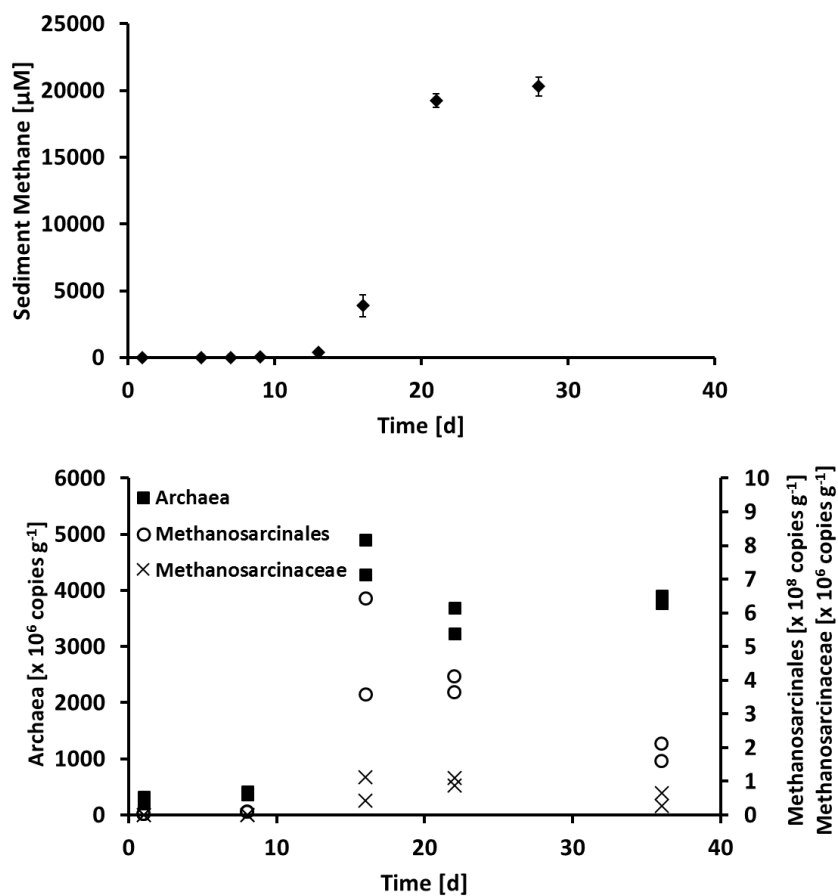
1222

1223

1224



1225 Figure 7



1226

1227

1228

1229

1230

1231

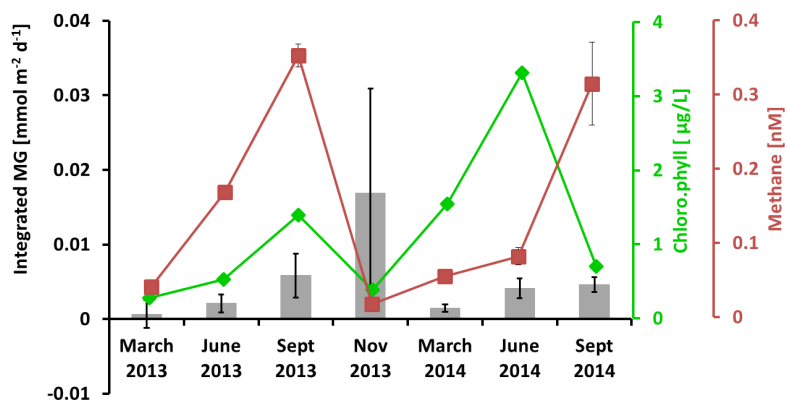
1232

1233

1234



1235 **Figure 8**



1236

1237

1238

1239

1240

1241

1242

1243

1244

1245

1246

1247

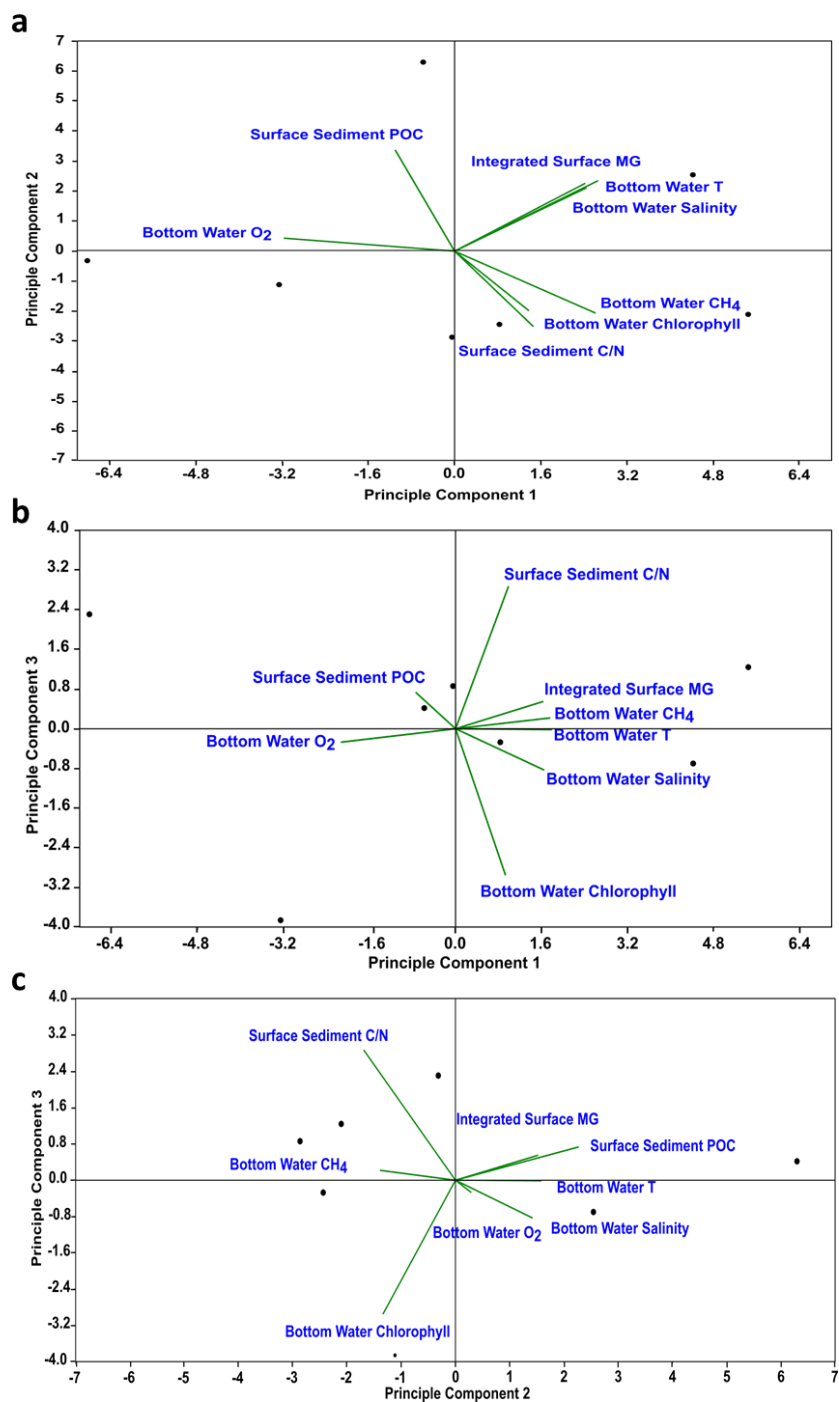
1248

1249

1250



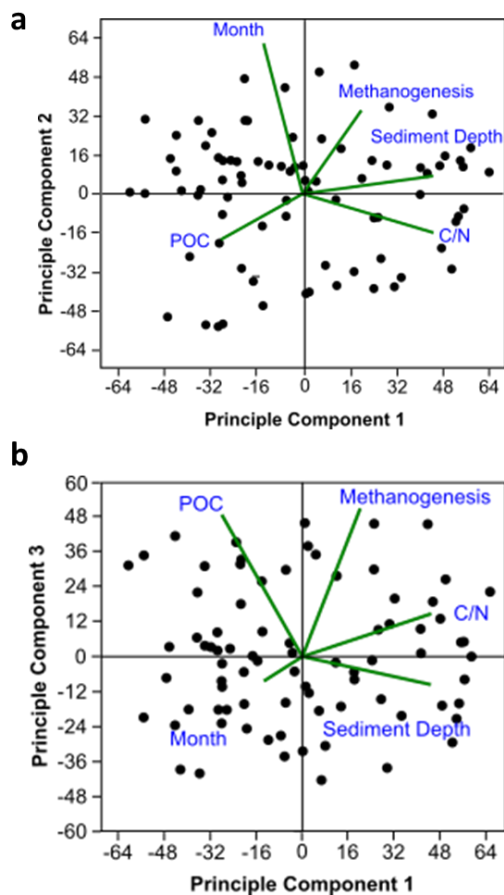
1251 **Figure 9**



1252



1253 **Figure 10**



1254

1255

1256

1257

1258

1259

1260

1261